

Charged Higgs decay to $W^\pm H$ at a high energy lepton collider

Majid Hashemi* and Laleh Roushandel†

Physics Department, College of Sciences, Shiraz University, Shiraz, 71946-84795, Iran

In this work, we present a search strategy for heavy charged Higgs boson at Compact Linear Collider (CLIC) as a future e^+e^- collider. The signal is charged Higgs boson pair production in two Higgs doublet model (2HDM) followed by $H^\pm \rightarrow W^\pm H$ and $H \rightarrow b\bar{b}$. Here, H denotes the heavy CP-even neutral Higgs boson of the model. The collider center of mass energy is chosen to be $\sqrt{s} = 1400$ GeV as the second stage of CLIC operation. In this case, $m_{H^\pm} < \sqrt{s}/2$ can be explored due to the pair production. It is shown that the signal of charged Higgs in the mass range $250 \text{ GeV} < m_{H^\pm} < 650 \text{ GeV}$ in fully hadronic final state, containing four b -jets from neutral Higgs and four jets from W bosons, can well be observed on top of the standard model background. Finally 5σ contours are presented in (m_{H^\pm}, m_H) space for different $\tan\beta$ values.

I. INTRODUCTION

During the last decades, standard model of particle physics (SM) has been tested with a reasonable precision and it has proved to be a satisfactory model of electroweak and strong interactions.

The Physics Nobel prize in 2013 was awarded to theoretical prediction of the Higgs boson [1–6] which had been experimentally confirmed by the two CMS and ATLAS collaborations of the Large Hadron Collider (LHC) experiment [7, 8].

Soon after observation of the new boson, extensive studies focused on its properties including production cross section, decay rates, couplings, spin, parity and CP structure [9–16]. There is overall agreement between the measured properties of the new boson with SM prediction.

There are, however, open problems which imply that the underlying theory of nature is beyond SM. There is a long list of such problems. One of the main issues is the so called hierarchy problem, i.e., finite mass of the observed Higgs boson which is theoretically sensitive to radiative corrections and the large difference between the electroweak scale and the Planck mass. One natural solution for the hierarchy problem is supersymmetry which requires an extended Higgs sector (at least two Higgs doublets) and reduces the divergence of radiative corrections to the Higgs boson mass without a fine tuning of the model parameters [17, 18].

Another main issue is the origin of dark matter (DM) discussed in a variety of theoretical models such as inert doublet model (IDM) [19–25], SM with a real [26–32] or complex scalar singlet [33–37] and supersymmetry [38]. The collider searches for the dark matter candidates are one of the main tasks in parallel with searches for extra Higgs bosons and supersymmetry [39, 40].

Other scenarios address the CP violation through baryon asymmetry at the electroweak scale [41] or the neutrino mass [42].

These beyond SM (BSM) scenarios all need extended Higgs sectors and can be built to predict and confirm the observed particle at LHC. In such a situation, the observed particle belongs to a family of Higgs bosons predicted in a more general model.

One of the most attractive BSM candidates is two Higgs doublet model (2HDM) which has been considered as a model of CP violation in its original form [43]. There is currently a high motivation for this model not necessarily as a basis for supersymmetry.

The Higgs sector of 2HDM incorporates two Higgs doublets resulting in five physical Higgs bosons [43–45], i.e., three neutral bosons (h , H , A) and two charged bosons (H^\pm) [46, 47].

The recently observed deviation of the W boson mass from SM prediction by the CDF collaboration [48] has imposed constraints on the 2HDM parameter space. The deviations in m_W had been explained in terms of singlet extension to SM [49] and 2HDM [50] before CDF announcement. However, there has been a large number of recent studies discussing the charged and neutral scalar mass splitting [51–56], and the interplay between the 2HDM and the muon $g-2$ anomaly in the light of the recent m_W measurement [57–61]. There are also studies which find upper limits of 1 TeV on the masses of the charged and neutral 2HDM scalars [62, 63].

In a CP conserving scenario without FCNC, there are four types of 2HDM in terms of Higgs-fermion diagonal couplings with a rich phenomenology [64, 65]. The type 2 serves as the basis to build the Higgs sector of the Minimal Supersymmetric SM (MSSM) [66–69].

In the so called alignment limit, one of the 2HDM neutral Higgs bosons (usually the lightest) acquires the same properties as those of the SM Higgs at tree level and plays the role of the LHC observation at 125 GeV [70–73]. The tree level alignment is however broken when loop corrections are included. Other 2HDM neutral Higgs bosons can have different properties (decay rates, CP, ...) which makes them distinguishable from the lightest boson especially at the decoupling limit which occurs if the mass difference between the SM-like Higgs boson (h) and heavy bosons is large [74, 75].

Observation of a new scalar is a signal for BSM with

* hashemi.mj@shirazu.ac.ir

† l.n.roushandel@gmail.com

extended Higgs sector. The signal of these scalars can be different in terms of their decay products and decay rates. If one of these scalars has SM-like couplings, the other one has couplings which are significantly different from the SM Higgs (e.g., no coupling to W and Z bosons). On the other hand, there is no elementary charged scalar in SM and observation of a charged Higgs with its unique signatures (electric charge, decay channels, ...) is a crucial proof that the underlying theory is beyond SM.

The charged Higgs bosons were used to explain the observed deviations of flavor physics observables from SM predictions in the past. These observables were $b \rightarrow s\gamma$ transition rate [76–79], branching ratio of heavy meson decay to $\tau\nu$ including $B_u \rightarrow \tau\nu$, $D_s \rightarrow \tau\nu$ [80] and $B_s \rightarrow \mu^+\mu^-$ [81–83]. These decays all contain diagrams involving charged weak currents which yield different results if charged Higgs boson contributions are added. A fine tuning of the model parameters achieves an agreement between 2HDM prediction and experimental observations better than SM [84]. The observed 2.4σ deviation in fully leptonic decays of B mesons reported in 2020 has recently reduced to less than 1σ below SM [85, 86]. Even in case of no deviation, these measurements impose strong constraints on 2HDM parameters [87, 88]. Currently $b \rightarrow s\gamma$ channel provides the strongest lower limit on m_{H^\pm} [76–79]. These studies are considered as indirect searches for new physics and are complementary to the direct searches at colliders [89].

Here we are going to focus on the Higgs sector of 2HDM and provide collider signatures which can be explored at future colliders for charged Higgs boson discovery. In what follows, a review of theoretical framework and collider searches for the charged Higgs and their current results is presented. After a discussion on different decay channels of the neutral and charged Higgs bosons, the charged Higgs decay to W^\pm boson and a heavy neutral Higgs boson is introduced as the search channel following previous studies using $H^+ \rightarrow t\bar{b}$ and $H^+ \rightarrow \tau^+\nu$. We present the analysis as a proposal for a future high energy e^+e^- collider which is specifically assumed to be CLIC in its second stage of operation [90]. We show that heavy charged Higgs mass region can well be probed at lepton colliders through $e^+e^- \rightarrow H^+H^-$ in the fully hadronic final state. Results show reasonable performance of such colliders compared to LHC.

II. THEORETICAL FRAMEWORK

The Higgs sector of the 2HDM Lagrangian is a natural expansion of SM to contain two complex scalar doublets with kinetic terms and the potential written in the form:

$$\mathcal{L}_\Phi^{2\text{HDM}} = \sum_{i=1,2} (D_\mu \Phi_i)^\dagger (D^\mu \Phi_i) - \mathcal{V}^{2\text{HDM}}. \quad (1)$$

The Higgs-gauge interaction terms are embedded in the kinetic term containing D_μ (the covariant derivative) and

the two doublets (Φ) are

$$\Phi_i = \begin{pmatrix} \phi_i^+ \\ (v_i + \rho_i + i\eta_i)/\sqrt{2} \end{pmatrix}, \quad i = 1, 2. \quad (2)$$

The neutral and charged Higgs fields are obtained by introducing two mixing angles α and β acting on the neutral and charged parts of the doublet containing ρ_i , η_i and ϕ_i^\pm through

$$\begin{aligned} h &= -\rho_1 \sin \alpha + \rho_2 \cos \alpha \\ H &= \rho_1 \cos \alpha + \rho_2 \sin \alpha \\ A &= \eta_1 \sin \beta + \eta_2 \cos \beta \\ H^\pm &= \phi_1^\pm \sin \beta + \phi_2^\pm \cos \beta. \end{aligned} \quad (3)$$

The ratio of vacuum expectation values of the two doublets is related to the mixing angle β through $\tan \beta = v_2/v_1$ under the conditions $v_1^2 + v_2^2 = v^2 = (246 \text{ GeV})^2$. At the alignment limit which occurs if $\sin(\beta - \alpha) = 1$ or $\beta - \alpha = \pi/2$, the β parameter determines the Higgs-fermion couplings [91].

The Higgs boson mass terms and Higgs self-interactions are formulated in the potential term which is written as follows:

$$\begin{aligned} \mathcal{V}^{2\text{HDM}} &= m_{11}^2 \Phi_1^\dagger \Phi_1 + m_{22}^2 \Phi_2^\dagger \Phi_2 - m_{12}^2 (\Phi_1^\dagger \Phi_2 + \Phi_2^\dagger \Phi_1) \\ &+ \frac{1}{2} \lambda_1 (\Phi_1^\dagger \Phi_1)^2 + \frac{1}{2} \lambda_2 (\Phi_2^\dagger \Phi_2)^2 \\ &+ \lambda_3 (\Phi_1^\dagger \Phi_1) (\Phi_2^\dagger \Phi_2) + \lambda_4 (\Phi_1^\dagger \Phi_2) (\Phi_2^\dagger \Phi_1) \\ &+ \frac{1}{2} \lambda_5 \left[(\Phi_1^\dagger \Phi_2)^2 + (\Phi_2^\dagger \Phi_1)^2 \right]. \end{aligned} \quad (4)$$

This form of the potential (up to a soft symmetry breaking term m_{12}) respects the Z_2 symmetry, i.e., invariance of the Lagrangian under interchange of $\phi_1 \rightarrow \phi_1$, $\phi_2 \rightarrow -\phi_2$ or $\phi_1 \rightarrow -\phi_1$, $\phi_2 \rightarrow \phi_2$ which prevents $\phi_1 \rightleftharpoons \phi_2$ transitions which result in CP violation [92]. Therefore the above form of the potential is the basis for a CP conserving 2HDM.

The Higgs-fermion couplings can be separated to the neutral Higgs interactions with fermions and the charged Higgs sector. The former has been studied in recent analyses extensively including our works on type 1 [93–96], type 3 [97–99] and type 4 [99–102]. In this analysis we focus on the charged Higgs search at a lepton collider with enough center of mass energy to explore high masses which have been out of LHC reach.

The charged Higgs interaction with fermions takes the following Lagrangian:

$$\begin{aligned} \mathcal{L} &= \frac{g}{2\sqrt{2}m_W} H^\pm [V_{ij} m_{u_i} \rho^u \bar{u}_i (1 - \gamma^5) d_j \\ &+ V_{ij} m_{d_j} \rho^d \bar{u}_i (1 + \gamma^5) d_j \\ &+ m_l \rho^l \bar{\nu}_i (1 + \gamma^5) l_i] + h.c. \end{aligned} \quad (5)$$

Model type \ Coupling	ρ^u	ρ^d	ρ^l
1	$\cot \beta$	$\cot \beta$	$\cot \beta$
2	$\cot \beta$	$-\tan \beta$	$-\tan \beta$
3	$\cot \beta$	$-\tan \beta$	$\cot \beta$
4	$\cot \beta$	$\cot \beta$	$-\tan \beta$

TABLE I: Higgs-fermion couplings in different types of 2HDM at the alignment limit.

where $v = 2m_W/g$, V_{ij} are CKM matrix elements and coupling factors ρ are given in Tab. I for each type of the 2HDM.

There are also charged Higgs decay to gauge bosons in the form of $H^\pm \rightarrow W^\pm \phi$ with $\phi = h/H/A$ as one of the neutral Higgs bosons. The vertices and decay rates of these channels are type independent as listed below:

$$\begin{aligned}
HH^+W^- &: \frac{g \sin(\beta - \alpha)}{2} \\
hH^+W^- &: \frac{g \cos(\beta - \alpha)}{2} \\
AH^+W^- &: \frac{ig}{2}.
\end{aligned} \tag{6}$$

However, the branching ratios depend on the 2HDM type due to dependence of other fermionic decay channels. At the alignment limit, with $\sin(\beta - \alpha) = 1$, $H^+ \rightarrow W^+h$ is suppressed while other decays. i.e., $H^+ \rightarrow W^+H$ and $H^+ \rightarrow W^+A$ can be significant if two conditions are satisfied.

The first condition is that the fermionic decays are suppressed. This suppression occurs for heavy charged Higgs decay $H^+ \rightarrow t\bar{b}$ at moderate $\tan \beta$ values which minimize the term $m_t \cot \beta + m_b \tan \beta$ for the $H^+t\bar{b}$ coupling in Eq. 5. This condition occurs in 2HDM types 2 and 3 at $\tan \beta = \sqrt{m_t/m_b} \simeq 6.5$. Other types disfavor $H^+ \rightarrow t\bar{b}$ at high $\tan \beta$ values.

The second condition is to have enough kinematic phase space for the decay. In MSSM-like 2HDM scenarios with degenerate masses for the Higgs bosons, these Higgs conversion decays are kinematically forbidden. It has been shown that for $\Delta\rho$ to be small enough and consistent with electroweak precision measurements, at least one of the heavy neutral Higgs bosons should have the same mass as the charged Higgs boson, i.e., $m_H = m_{H^+}$ or $m_A = m_{H^+}$ [103–106]. The second option is adopted in this analysis leading to the mass spectrum $m_h < m_H < m_A (= m_{H^+})$. Therefore $H^+ \rightarrow W^+A$ is naturally suppressed and the only remaining non-fermionic decay is $H^+ \rightarrow W^+H$. We will describe the analysis of this channel in details after a brief review of the past and recent searches for the charged Higgs boson in different decay channels in the next section.

III. REVIEW OF THE CURRENT RESULTS

The charged Higgs searches have been historically divided into two main categories of light ($m_{H^+} \lesssim m_t$) and heavy ($m_{H^+} \gtrsim m_t$) regions. Each region has its own characteristics which is described briefly.

A. Light charged Higgs

The light charged Higgs can be produced in top quark decay through $t \rightarrow H^+b$ and competes with SM decay $t \rightarrow W^+b$. In the absence of charged Higgs boson, the top quark branching ratio of decay to W is close to unity. However, in certain circumstances, e.g., when the coupling factor, ρ^d in the second term of Lagrangian (Eq. 5) is large, $t \rightarrow H^+b$ decay rate can be significant. This situation occurs in 2HDM types 2 and 3 where $\rho^d = -\tan \beta$ and enhances at high $\tan \beta$ values. Since the main decay channels in this case are $t \rightarrow W^+b$ and $t \rightarrow H^+b$ and sum of their branching ratios has to be unity, enhancement of ($t \rightarrow H^+b$) decay rate as $\tan^2 \beta$ leads to suppression of ($t \rightarrow W^+b$). One has to note that enough phase space is also required for significant decay rate and m_{H^+} values close to the top quark mass result in suppression of non-SM decay $t \rightarrow H^+b$. When the light charged Higgs is produced in top quark decay, usually $H^+ \rightarrow \tau^+\nu$ is analyzed because $H^+ \rightarrow t\bar{b}$ is kinematically suppressed. The τ lepton in its hadronic decay produces a sharp signature for the charged Higgs boson due to the mass difference between H^+ and W^+ , and spinless nature of the charged Higgs boson compared to the case of spin-1 W boson. These effects have been discussed extensively in the literature [107–113].

The charged Higgs boson production through the top quark decay ($t \rightarrow H^+b$) and its decay to τ jet ($H^+ \rightarrow \tau^+\nu$) has been the search channel from the time of LEP [114–116] to TeVatron collaborations D0 [117–120] and CDF [121–123]. The preliminary studies at LHC [124, 125] were followed by CMS [126, 127] and ATLAS [128, 129] using 7 TeV data. The 8 TeV results were then reported by CMS [130] and ATLAS [131]. Currently the light charged Higgs masses below 160 GeV are excluded for all $\tan \beta$ values in MSSM (which is based on 2HDM type 2) as reported by 13 TeV LHC data analyses [132, 133].

B. Heavy charged Higgs

If the charged Higgs boson is heavier than the top quark, it can not be produced in on-shell top quark decays. The off-shell production of the top quarks can instead be used to produce the charged Higgs bosons. The light charged Higgs production process which is $pp \rightarrow t\bar{t}$ at LHC, with at least one of the top quarks decaying to the charged Higgs, is replaced by $pp \rightarrow t\bar{b}H^-$ whose cross

section calculation was performed in several works before the LHC startup [134–138].

In the heavy charged Higgs region there is still possibility to adopt $H^+ \rightarrow \tau^+\nu$ for the search, especially in 2HDM types 2 and 4 which allow enhancement of the charged Higgs leptonic decay with its decay rate being proportional to $\tan^2\beta$.

The alternative decay channel is $H^+ \rightarrow t\bar{b}$ which benefits from a larger mass term in the vertex (m_b vs. m_τ) and can be significant in 2HDM types 2 and 3 with the same reasons as discussed about $t \rightarrow H^+b$ previously. This channel has already been studied in the literature [139–146] followed by LHC results reported by ATLAS [147, 148] and CMS collaborations [149, 150] which excluded charged Higgs masses above 200 GeV for $\tan\beta$ values below 2.1 and also above 34.

The analysis of the charged Higgs decay to $c\bar{s}$ has also been recently reported by CMS collaboration [151]. The off-diagonal decay to $c\bar{b}$ has been analyzed by CMS [152] and ATLAS collaborations [153, 154] with their results reported as upper limits on the product of production cross section times branching ratio of the light charged Higgs decay.

Other decay channels have also been proposed such as $H^+ \rightarrow \mu^+\nu$ [155, 156].

It should be noted that the final state of $H^+ \rightarrow t\bar{b}$ with $t \rightarrow W^+b$ and $W \rightarrow jj$ is the same as $H^+ \rightarrow W^+H$ followed by $W \rightarrow jj$ and $H \rightarrow b\bar{b}$. These two modes can be comparable with large branching ratios in the region near $\tan\beta \sim 7$ as discussed extensively in [157].

In the context of 2HDM type 1, the charged Higgs bosonic decays have been studied in [158]. The charged Higgs- W boson coupling involved in $pp \rightarrow H^\pm\phi$ production at LHC with $\phi = h/H/A/W^\mp$ together with decays with the same vertices involved are discussed in [159] with several benchmark scenarios introduced for LHC searches. The same type of charged Higgs associated production with $\phi = h/A$ or H^+H^- pair production with $H^\pm \rightarrow W^\pm h/A$ have been discussed in [160] and the regions of parameter space where the charged Higgs bosonic decays are enhanced are identified.

An analysis of $H^\pm \rightarrow W^\pm h_{125}$ has been proposed for LHC in [161]. The loop contributions to $H^\pm \rightarrow W^\pm V$ ($V = \gamma/Z$) has been calculated in [162] leading to one to three orders of magnitude enhancement in those branching ratios. A proposal for the energy upgrade of LHC to probe $H^\pm W^\mp Z$ interaction has been presented in [163].

The CMS collaboration has reported their first results of heavy charged Higgs search by analyzing $H^+ \rightarrow W^+H$ [164]. They have set upper limits on the cross section times $\text{BR}(H^+ \rightarrow W^+H)$ for the charged Higgs masses above 300 GeV and the heavy CP-even neutral Higgs mass fixed at $m_H = 200$ GeV. The analysis of $H^+ \rightarrow W^+A$ has also been reported for a light charged Higgs in the mass range $100 \text{ GeV} < m_{H^+} < 160 \text{ GeV}$ [165, 166].

The $H^+ \rightarrow W^+Z$ has been searched for by CMS [167] and ATLAS [168, 169] collaborations. The multi-lepton final state of the charged Higgs decay to vector boson has

been reported in [170].

Despite the extensive search for the charged Higgs bosonic decays, a large region of the parameter space is still unexplored and will be shown to be out of HL-LHC reach too.

IV. ANALYSIS OF $H^+ \rightarrow W^+H \rightarrow jjbb$ AT CLIC

A. Collider choice

There are different scenarios for the future of colliders in hadron-hadron and lepton-lepton collision modes. The Large Hadron Collider (LHC) after an upgrade is going to operate in high luminosity mode HL-LHC [171, 172]. The new design as Future Circular Collider is going to be the next generation collider operating in two modes of hadronic collisions with $\sqrt{s} = 100$ TeV as FCC-hh [173], and e^+e^- collisions with $\sqrt{s} = 350$ GeV as FCC-ee in top factory mode [174, 175]. There are other proposals such as International Linear Collider (ILC) [176–178] operating at $\sqrt{s} = 500$ GeV and CEPC [179, 180] with $\sqrt{s} = 240$ GeV.

The above hadron collision programs will follow LHC in their luminosity and energy frontier [181]. In lepton collision modes there have been numerous studies of lepton colliders and their potential for Higgs boson searches at ILC [182] and CEPC [183]. However, a suitable choice for heavy Higgs boson searches is Compact Linear Collider (CLIC) in its high energy operation modes (stages 2 and 3 with $\sqrt{s} = 1400$ and 3000 GeV respectively) [184, 185]. The first stage of CLIC operation will be at $\sqrt{s} = 350$ GeV and can not be used for heavy Higgs boson searches targeted in this work. Therefore the first realization of a lepton collider providing the opportunity to search for charged Higgs bosons in pair production with masses above 200 GeV occurs at the second stage of CLIC at $\sqrt{s} = 1400$ GeV. This is the collider choice for the analysis which will be described in this paper. The ultimate operation mode can be reserved to focus on unexplored regions of the 2HDM parameter space which escaped from the previous stages.

B. Software setup

The branching ratios of neutral and charged Higgs bosons as well as theoretical constraints are obtained using 2HDMC-1.8.0 [186–188]. The experimental exclusion regions are obtained using HiggsTools-1 [189]. The cross section and event generation is performed with the use of WHIZARD-3.1.2 [190, 191] which benefits from beam spectra for lepton colliders using subpackage circe2 [192]. Events containing hard scattering are passed to PYTHIA-8.3.09 [193] for multi-particle interactions and final state radiation and showering. The detector simulation is performed using DELPHES-3.5.0 [194–196]. The detector card CLICdet.Stage2 is used

to perform the physical object reconstruction including jet reconstruction and flavor association, b -tagging (in 90% efficiency scenario) including fake rate (p_T and θ dependent), charged track and jet momentum smearing [197–199]. The final result visualization is done using ROOT-6.28 [200] and python3 libraries numpy [201] and matplotlib [202].

C. Theoretical constraints

The Higgs sector potential in Eq. 4 is subject to theoretical requirements of positivity (being bounded from below) [75, 203–206], unitarity (of the scattering S-matrix) and perturbativity (in the Higgs quartic interactions) [92, 207, 208] and $\Delta\rho$ (to be within the range of electroweak precision measurements) [103–106].

The benchmark points considered in this work fall in the range $250 \text{ GeV} < m_{H^+} < 650 \text{ GeV}$. The signal cross section with heavier charged Higgs bosons tends to zero when reaching $m_{H^+} \rightarrow \sqrt{s}/2$. For each charged Higgs mass, the neutral CP-even Higgs boson mass is selected from the range $150 \text{ GeV} < m_H < 550 \text{ GeV}$. Both mass increments are 100 GeV and the minimum mass difference between m_H and m_{H^+} has to be 100 GeV. The CP-odd Higgs boson mass is equal to the charged Higgs mass as stated in section II. The analysis is presented for $\tan\beta = 10$ which is close to the excluded region of neutral Higgs boson in 2HDM type 3.

The above theoretical requirements are satisfied for all points except for the point $(m_{H^+}, m_H) = (650, 150) \text{ GeV}$ where only positivity, unitarity and $\Delta\rho$ requirements are satisfied. Although the signal process does not involve $2 \rightarrow 2$ Higgs interactions which are verified by perturbativity requirement, all theoretical considerations have to be taken into account for the potential to be physically sensible. However, we keep this point in the list for completeness of the search domain which is available at this center of mass.

D. Neutral Higgs boson considerations

The current analysis is going to focus on the heavy charged Higgs search through $H^+ \rightarrow W^+H$. Therefore it is more relevant to (but still different from) the CMS analysis reported in [164] where the final state is obtained via $H^+ \rightarrow W^+H$ followed by $H \rightarrow \tau\tau$ with at least one of the τ leptons decaying hadronically. It is based on obtaining the distribution of charged Higgs transverse mass after a reasonable treatment of the missing transverse energy originated from hadronic decays of τ leptons, τ tagging as well as top quark tagging as the production process in their case is $pp \rightarrow t\bar{b}H^-$.

These event characteristics are different from what we are going to propose in the current work. In fact, in 2HDM types 1 and 3, the relevant decay mode for the heavy neutral Higgs boson is $H \rightarrow b\bar{b}$ as shown in Fig.

1. In type 1, $H \rightarrow b\bar{b}$ is suppressed if $m_H \gtrsim 2m_t$ but in that region the dominant decay channel is $H \rightarrow t\bar{t}$ which produces a large final state particle multiplicity and a signal discrimination from the background will be challenging. The other 2HDM types 2 and 4 are highly excluded by the current experimental searches at LHC or will be covered at high luminosity LHC (HL-LHC) as shown in Fig. 2.

The HL-LHC exclusion region expectation is obtained by statistical extrapolation of current results from CMS and ATLAS to integrated luminosity of $\mathcal{L}_{\text{HL-LHC}} = 3000 \text{ fb}^{-1}$ per experiment leading to total $\mathcal{L} = 6000 \text{ fb}^{-1}$ [172]. In order to do so, the current signal ratios in HiggsBounds datasets are scaled by a factor of $\sqrt{\mathcal{L}_{\text{current}}/\mathcal{L}_{\text{HL-LHC}}}$ where the current integrated luminosity is taken from the dataset file.

According to Fig. 2, lower limits of 250 and 350 GeV are set on the neutral Higgs masses based on the current LHC exclusion and HL-LHC expectation for both 2HDM types 1 and 3 with $\tan\beta < 10$.

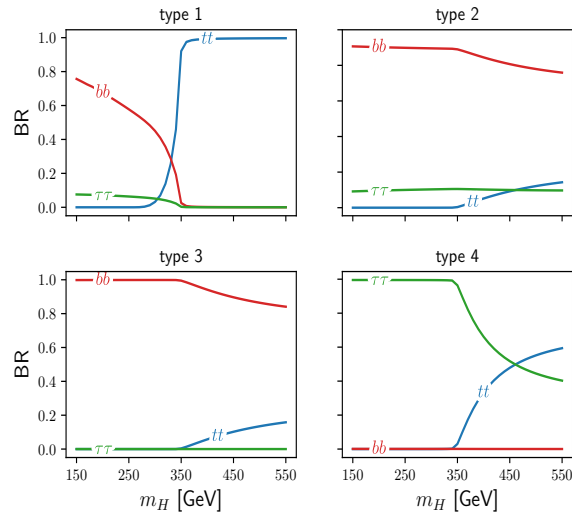


FIG. 1: The neutral Higgs boson branching ratio of decay to different final states $b\bar{b}$, $\tau^+\tau^-$ and $t\bar{t}$ as a function of the Higgs boson mass at $\tan\beta = 10$ in different types of 2HDM.

The analysis to be presented is limited to 2HDM types 1 and 3 in $4b$ final state. The 2HDM type 4 is left due to the possibility of coverage by HL-LHC and lower efficiency of τ -tagging compared to b -tagging. The τ -tagging efficiency at CLIC in the transverse momentum range $50 \text{ GeV} < p_T < 125 \text{ GeV}$ is $\sim 60\%$ [215], while the b -tagging efficiency can be as high as 90% [216].

E. Charged Higgs boson considerations

The charged Higgs boson is pair produced at e^+e^- collisions through $e^+e^- \rightarrow \gamma/Z/h/H \rightarrow H^+H^-$. The

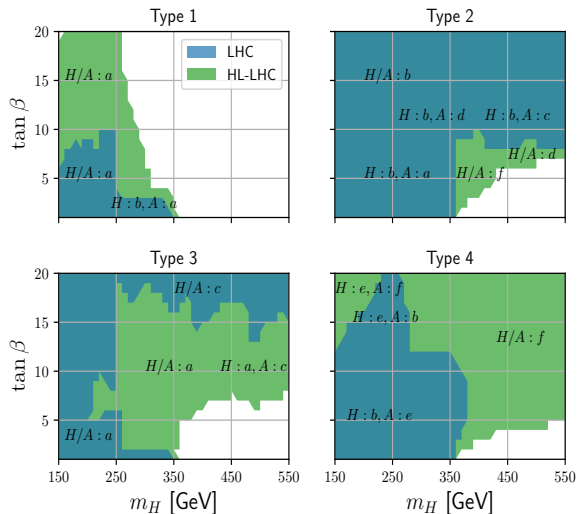


FIG. 2: The 95% C.L. excluded regions of the heavy neutral Higgs bosons shown in blue (LHC) and green (HL-LHC expectation) as a function of the Higgs boson mass vs. $\tan\beta$. Labels show the corresponding analyses with highest sensitivity for CP-even H and CP-odd A exclusion: a: $A \rightarrow ZH$ [209], b: $\phi \rightarrow \tau\tau$ [210], c: $jj\gamma$ [211], d: $\phi \rightarrow \tau\tau$ [212], e: $H/A \rightarrow ZA/H$ [213], f: $\phi \rightarrow \tau\tau$ [214] ($\phi = h/H/A$).

contribution from neutral Higgs bosons in the s -channel propagator is negligible due to the low Higgs-electron coupling. The process is thus effectively Drell-Yan event (with incoming e^+e^-) producing off-shell photon or Z boson [217, 218] which produce a charged Higgs boson pair. As mentioned before the two modes $H^+ \rightarrow t\bar{b}$ and $H^+ \rightarrow W^+H$ produce the same final states if $H \rightarrow b\bar{b}$. The branching ratio of charged Higgs boson decay in these channels are shown in Figs. 3 and 4. Assuming the minimum mass for the neutral Higgs boson as 150 GeV, charged Higgs boson masses above 250 GeV are considered so that $H^+ \rightarrow W^+H$ is kinematically allowed.

The LHC excluded regions at 95% CL and HL-LHC exclusion expectation are shown in blue and green respectively in Figs. 3 and 4.

The light charged Higgs exclusion extends to the top mass threshold by $H^+ \rightarrow \tau\nu$ search at HL-LHC in types 2 and 4 where the leptonic decay is relevant. The heavy charged Higgs region at high $\tan\beta$ values will be covered by $H^+ \rightarrow \tau\nu$ search in type 2 and $H^+ \rightarrow t\bar{b}$ in type 3 (in this type the leptonic decay is suppressed at high $\tan\beta$). The very low $\tan\beta$ regions show normal extensions of the three analyses a, b, c when HL-LHC data is available. Therefore the region $\tan\beta \gtrsim 3$ is out of HL-LHC reach in type 1, while in type 3, the allowed region will be $3 \lesssim \tan\beta \lesssim 13$.

As seen from Figs. 3 and 4, in 2HDM type 1, at $\tan\beta = 10$, $H^+ \rightarrow t\bar{b}$ contributes 15% to 40% of the charged Higgs decay and the rest of 60% to 85% be-

longs to $H^+ \rightarrow W^+H$. In type 3, the situation is in favor of $H^+ \rightarrow t\bar{b}$ absorbing 45% to 73% of the total decay fraction while the rest of 27% to 55% is taken by $H^+ \rightarrow W^+H$. Other types of the model are not considered due to neutral Higgs exclusions as shown in Fig. 2.

The charged Higgs loop contribution in the $h_{125} \rightarrow \gamma\gamma$ decay rate is also evaluated by passing decay rates from 2HDMC to HiggsSignals for the model χ^2 evaluation. The analysis shows preference of heavy charged Higgs bosons as discussed in [159]. The $h_{125} \rightarrow \gamma\gamma$ involves $\gamma H^+ H^-$ coupling which is the electric charge and $h_{125} H^+ H^-$ coupling which is $-\frac{1}{v}[m_{h_{125}}^2 + 2(m_{H^\pm}^2 - m^2)]$ at the alignment limit with $m^2 = m_{12}^2/(\sin\beta \cos\beta)$ which is set to $m_{H^\pm}^2$ as suggested in [73] for alignment scenario. The two couplings are thus independent of the model type and α, β parameters. Taking minimum χ^2 corresponding to $m_{H^\pm} = 1$ TeV as the reference, $\Delta\chi^2$ is obtained in the charged Higgs mass and $\tan\beta$ parameter space and 68% and 95% CL bounds are drawn as vertical blue lines on the top left panel in Fig. 3. The observation is that the region of study $m_{H^\pm} \gtrsim 250$ GeV is within the LHC bound from $h_{125} \rightarrow \gamma\gamma$ rate at 95% CL.

The HL-LHC expectation is estimated using projected uncertainties reported by CMS and ATLAS in Tab. 35 of [171] for h_{125} decay channels. The uncertainties from the second scenario, S2, also called YR18, are implemented in HiggsSignals for the model χ^2 evaluation. The lower limits for the charged Higgs mass are obtained as 700 GeV (95% CL) and 850 GeV (68% CL) as expected by HL-LHC.

Considering the charged Higgs boson pair production at e^+e^- collisions, the signal cross section is multiplied by square of $\text{BR}(H^+ \rightarrow W^+H) \cdot \text{BR}(H \rightarrow f\bar{f})$ as shown in Fig. 5. Here, f is b in types 1 to 3, and τ in type 4. In type 1, $\sigma \cdot \text{BR}$ values decrease to below 0.1 fb at masses above 450 GeV due to smallness of $\text{BR}(H \rightarrow b\bar{b})$. The observed patterns in the four types reflect the fact that there is a mass splitting between the charged and neutral Higgs bosons allowing $H^+ \rightarrow W^+H$ decay.

F. Search strategy

1. Cut based analysis

The signal in fully hadronic final state contains a total number of eight jets. Figure 6 shows a typical signal event in two views of a general detector concept. For event analysis, we require that there are at least eight reconstructed jets in the event using the Valencia jet reconstruction algorithm [219, 220]. The kinematic acceptance for jets is

$$p_T > 5 \text{ GeV and } |\eta| < 5 \quad (7)$$

with the usual transverse momentum and pseudorapidity definitions. A jet smearing is applied to mimic the $\gamma\gamma \rightarrow$

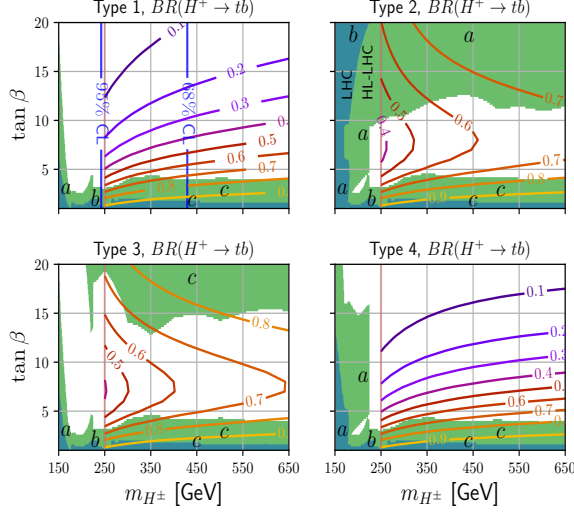


FIG. 3: The charged Higgs branching ratio of decay to $t\bar{b}$ as a function of the mass and $\tan\beta$ in different types of 2HDM. The blue and green regions show the LHC 95% C.L. excluded region and HL-LHC expectation respectively. Labels show the corresponding analyses with highest sensitivity: a: ATLAS $H^+ \rightarrow \tau\nu$ [133], b: ATLAS $H^+ \rightarrow t\bar{b}$ [148] and c: CMS $H^+ \rightarrow t\bar{b}$ [149]. The neutral Higgs boson mass is set to $m_H = m_{H^+} - 100$ GeV. The vertical blue lines show the lower limit of the charged Higgs boson mass within 68% and 95% CL bound from $h_{125} \rightarrow \gamma\gamma$ measurement at LHC.

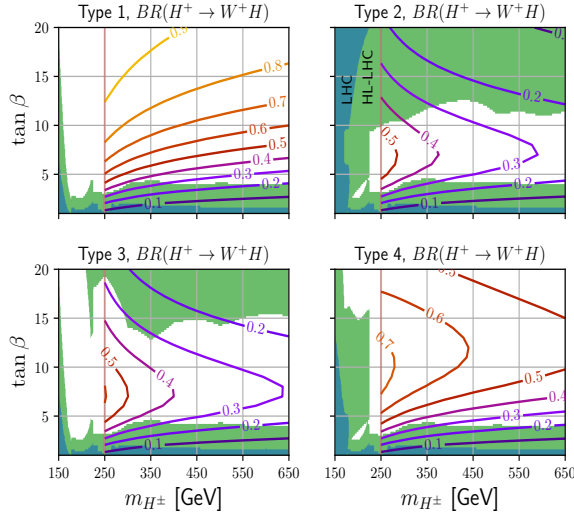


FIG. 4: The charged Higgs branching ratio of decay to WH as a function of the mass and $\tan\beta$ in different types of 2HDM. The neutral Higgs boson mass is set to $m_H = m_{H^+} - 100$ GeV.

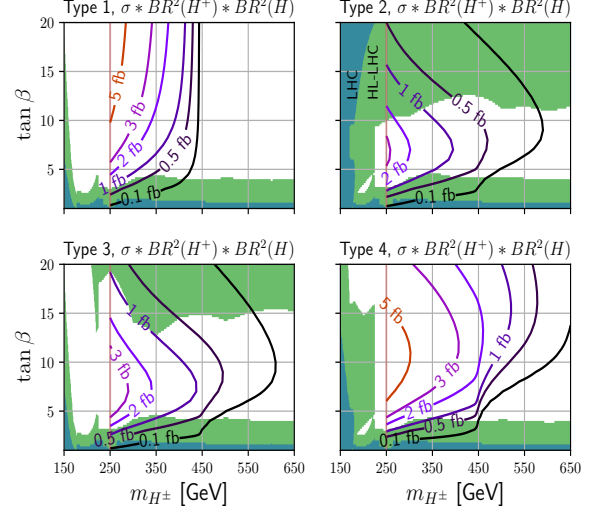


FIG. 5: The cross section times branching ratio of $e^+e^- \rightarrow H^+H^- \rightarrow W^+HW^-H \rightarrow W^+W^-ffff$ ($f = b$ in types 1 to 3, and τ in type 4) as a function of the charged Higgs mass and $\tan\beta$ in different types of 2HDM.

hadrons overlay as follows:

$$\frac{\delta p}{p} = \begin{cases} 0.01, & |\eta| < 0.76 \\ 0.05, & |\eta| \geq 0.76, \end{cases} \quad (8)$$

i.e., 1% and 5% smearing with Gaussian profile is applied on the jet four-momentum in the corresponding η regions. This is based on CLIC collaboration early proposal [198]. The distributions of jet multiplicity are shown in Figs. 7 (for the signal events with $(m_{H^\pm}, m_H) = (350, 150)$ GeV as an example) and 8a, 8b for $t\bar{t}$, $t\bar{t}b\bar{b}$ background events respectively.

As seen, in average, there are equal number of light and b -jets in signal events leading to total number of eight jets. In the $t\bar{t}$ background events, in average, there are two b -jets from the top quark decay and four light jets from W^\pm decays leading to total number of six jets. The $t\bar{t}b\bar{b}$ background produces similar jet multiplicities as in signal events due to the existence of 4 b -jets and total number of 8 jets in the final state.

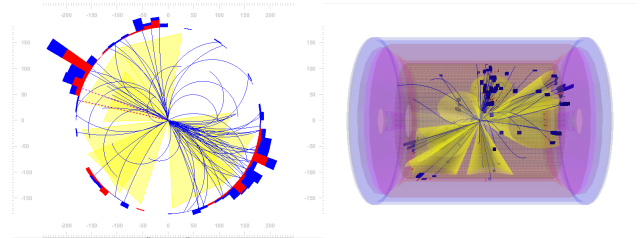


FIG. 6: A signal event containing 8 reconstructed jets in two views of the cylindrical coordinates.

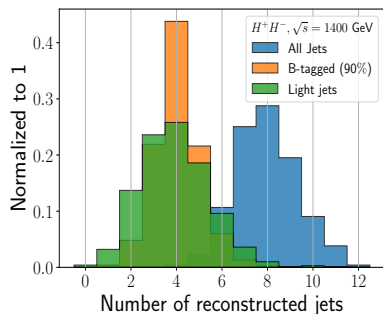


FIG. 7: Number of b -jets, light jets and total number of jets in signal events.

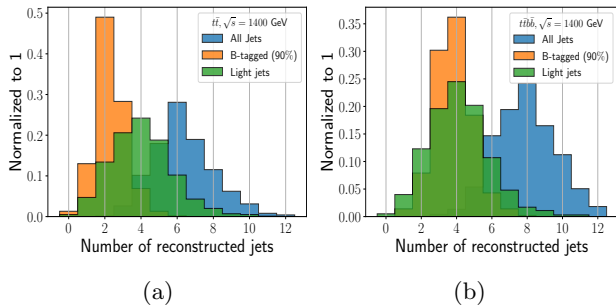


FIG. 8: Number of b -jets, light jets and total number of jets in $t\bar{t}$ (a) and $t\bar{t}b\bar{b}$ events (b).

In the next step, the W^\pm reconstruction is performed by searching for the correct pairs of light jets which minimize the following χ :

$$\chi = |m_{ij} - m_W| + |m_{kl} - m_W|, \quad (9)$$

where i, j, k, l are light jets indices, m_W is the W^\pm boson mass set to 80 GeV and m_{ij}, m_{kl} are invariant masses of the two pairs of light jets. When the best pairs of light jets are obtained through the above requirement, their invariant masses (labeled as m_{W1} and m_{W2}) are required to be around the nominal value of the W boson mass within 20 GeV window, i.e.,

$$|m_{W1} - m_W| < 20 \text{ GeV and } |m_{W2} - m_W| < 20 \text{ GeV}. \quad (10)$$

The procedure for heavy neutral Higgs boson reconstruction is very similar to that used for W boson except that the search proceeds among b -jets with indices i, j, k, l minimizing χ defined as:

$$\chi = |m_{ij} - m_H| + |m_{kl} - m_H|, \quad (11)$$

followed by the mass window:

$$|m_{H1} - m_H| < m_H/4 \text{ and } |m_{H2} - m_H| < m_H/4. \quad (12)$$

The χ minimization and subsequent mass window for the heavy neutral Higgs boson relies on the knowledge of its mass, m_H . Therefore it is assumed that this particle

has already been observed at the time of search for the charged Higgs boson through this analysis. Contrary to the case of W reconstruction, a dynamic mass window has been used for H reconstruction due to different mass hypotheses. The mass hypothesis here will be replaced by experimental input in case of successful observation of heavy neutral Higgs boson. The invariant mass distributions of reconstructed W/H bosons are shown in Fig. 9 before the mass windows are applied. The neutral Higgs boson invariant mass distribution becomes wider for higher masses as shown in Fig. 10.

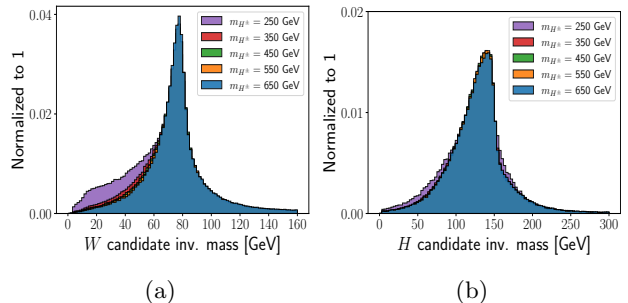


FIG. 9: Invariant mass distributions of the reconstructed W bosons (a) and H bosons with $m_H = 200$ GeV (b) in signal events producing different charged Higgs boson masses.

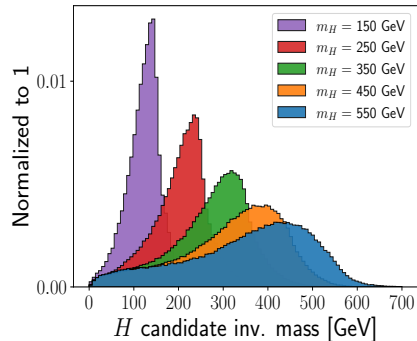


FIG. 10: The neutral Higgs boson invariant mass distributions for $150 \text{ GeV} < m_H < 550 \text{ GeV}$.

At this step, there are two pairs of light jets passed Eqs. 9, 10 with their invariant masses denoted as m_{IJ}^W and m_{KL}^W . The corresponding pairs of b -jets have passed Eqs. 11, 12 with m_{IJ}^H and m_{KL}^H as their invariant masses. The light and b -jet indices are obviously different. However, we use the same letters to avoid complexity in writing.

Before proceeding to the charged Higgs boson reconstruction, the jet four-momenta are corrected to give the correct invariant mass equal to the nominal value of the W^\pm or H bosons. This correction can be written in the following form:

$$p_{I,J}^\mu \rightarrow p_{I,J}^\mu * \frac{m_{W/H}}{m_{IJ}}, \quad (13)$$

where $\mu = 0$ to 3 are the four-momentum indices, I, J are the jet pair indices and the correction is performed for each value of I, J found in the previous step by χ minimization. The same correction is applied on jets with indices K, L .

The corrected light and b -jets are then used to construct the W/H four-momenta leading to W_1, W_2, H_1, H_2 with their invariant masses equal to m_W/m_H precisely. These are the four objects of the final state which can be used to reconstruct the charged Higgs bosons H^\pm . Let us call them FS_i , with $i = 1$ to 4 after sorting them in descending energy. A view of signal event is shown in Fig. 11.

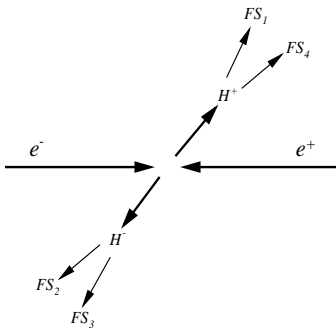


FIG. 11: A signal event containing two charged Higgs bosons with four final state objects FS_i denoting W/H bosons.

The pairing of the final state objects is performed by obtaining invariant masses $m_{(FS_1, FS_4)}$ and $m_{(FS_2, FS_3)}$. The idea is based on energy/momentum conservation which implies $\vec{p}_{H^+} = -\vec{p}_{H^-}$ and $E_{H^+} = E_{H^-} = \sqrt{s}/2$ leading to $E_{FS_1} + E_{FS_4} = E_{FS_2} + E_{FS_3} = \sqrt{s}/2$. Therefore the final state objects with the highest and lowest energies belong to the same mother particle (charged Higgs). The indices in Fig. 11 are thus selected so as to agree with the expectation.

In order to keep statistics of the signal events, we keep both combinations and fill the final invariant mass histograms with both $m_{(FS_1, FS_4)}$ and $m_{(FS_2, FS_3)}$ for double statistics.

2. Alternative approach

There are other methods for the signal event reconstruction. Since there are two corrected W and two H bosons, denoted by W_1, W_2, H_1, H_2 , the only possibilities for combining them and reconstructing the charged Higgs are $W_1 + H_1 \rightarrow H_1^+$, $W_2 + H_2 \rightarrow H_2^+$ or $W_1 + H_2 \rightarrow H_1^+$, $W_2 + H_1 \rightarrow H_2^+$. One can choose the pair of combinations which give closest charged Higgs boson masses and yield $\min\Delta(m_{H_1^+}, m_{H_2^+})$. This strategy was also studied leading to similar results to what already presented in the paper.

3. Likelihood analysis

The signal search strategy described here relies on cut-based counting experiment which applies dynamic mass windows on the final invariant mass distributions. An alternate approach is based on binned histogram extended likelihood analysis. In order to do so, the signal and background (invariant mass) histograms are used to get probability density functions (pdfs) of the distributions. Based on these pdfs, pseudo-data are generated and a profile likelihood is calculated for hypothesis tests. The signal significance is then obtained by comparing the null hypothesis (background only, no signal events) with the alternate hypothesis of signal plus background. Example of a signal ($(m_{H^+}, m_H) = (450, 150)$ GeV in type 3) and background model and generated data are shown in Fig. 12.

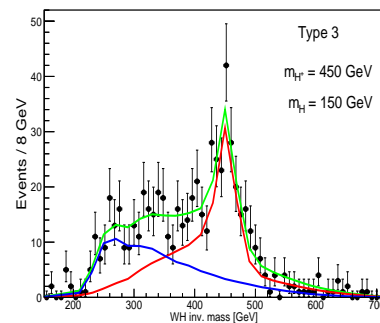


FIG. 12: The pseudo-data (markers with error bars) generated based on pdfs of the signal (red line) and total background (blue line). The signal plus background pdf is shown in green.

V. RESULTS

Figure 13 shows the charged Higgs invariant mass distributions in 2HDM types 1 and 3 with different charged and neutral Higgs boson mass hypotheses. The value of $\tan\beta$ is set to $\tan\beta = 10$. All distributions are normalized to integrated luminosity $\mathcal{L} = 1000 \text{ fb}^{-1}$. The $t\bar{t}$ background (shown in dark gray) has a total cross section of 145 fb . The $t\bar{t}b\bar{b}$ background which contains $t\bar{t}Z$ and $t\bar{t}h_{125} \rightarrow b\bar{b}$ followed by $Z/h_{125} \rightarrow b\bar{b}$ is shown in light gray and has a cross section of 3.8 fb . Other SM backgrounds ($Z/\gamma, ZZ, W^+W^-, b\bar{b}b\bar{b}$) have no contribution after jet multiplicity and b -tagging requirements. The red arrows show the mass window which provides the maximum signal significance defined as $N_S/\sqrt{N_S + N_B}$ where $N_S(N_B)$ is the signal(background) number of events in the final histogram within the mass window. The signal significance results for both cases of cut based and likelihood analyses are shown in Fig. 14.

In 2HDM type 1, as Fig. 5 indicates, the signal

cross section times branching ratio of charged and neutral Higgs boson decays is almost independent of $\tan\beta$ for $\tan\beta \geq 10$. Therefore results of the type 1 at $\tan\beta = 10$ are valid for higher $\tan\beta$ values. On the other hand, the neutral Higgs boson decay to $t\bar{t}$ which is activated at $m_H \geq 2m_t$, limits the region of parameter space to large mass splitting above 100 GeV for $m_{H^+} > 450$ GeV as $m_H^{\max} \simeq 350$ GeV for $H \rightarrow b\bar{b}$. Possibility of $H^+ \rightarrow W^+H$ with $H \rightarrow t\bar{t}$ should then be explored using top tagging techniques based on jet substructure [221] demanding four (fat) top jets to be found in the event [222–224]. Due to the top quark jet substructure in hadronic decay mode and the large jet multiplicity in signal events (16 jets), exploring the region of $m_{H^+} > 450$ GeV and $m_H > 350$ GeV is challenging in 2HDM type 1.

In 2HDM type 3, a broader region is accessible with $\sigma \times \text{BR}$ decreasing as m_{H^+} increases. There is $\tan\beta$ dependence in final results in this case and the best region is near $\tan\beta = \sqrt{m_t/m_b} \simeq 6.5$ which is where $H^+ \rightarrow t\bar{b}$ is suppressed as mentioned before. The $\tan\beta$ values below or above this region lead to reduction in $\text{BR}(H^+ \rightarrow W^+H)$ resulting in less signal rate.

Other types, are limited by neutral Higgs boson exclusions as shown in Fig. 2. In type 2, a heavy neutral Higgs boson can be used for the signal search in $H \rightarrow b\bar{b}$ mode at $\tan\beta < 5$ with masses above 350 GeV, but these masses are covered partially by HL-LHC. The type 4 is suitable with $H \rightarrow \tau\tau$ again at small region of $\tan\beta < 5$ which looks out of HL-LHC reach. The analysis of this type should be similar to what has already been done at LHC [164] keeping in mind the different nature of events and experiments.

Since final results depend on the m_{H^+}, m_H and $\tan\beta$, a scan over the parameter space of interest is performed to visualize the 5σ contours in types 1 and 3. Results

are shown in Fig. 15 as a function of the charged and neutral Higgs bosons for different $\tan\beta$ values below 10. The LHC neutral Higgs boson excluded region at 95% CL as well as HL-LHC expectation are also shown in Fig. 15.

VI. CONCLUSIONS

A search strategy for heavy charged Higgs boson decay to $W^\pm H$ was described as a proposal for a high energy lepton collider. The analysis was performed assuming CLIC operation at $\sqrt{s} = 1400$ GeV with fast detector simulation including parametrized b -tagging algorithm, jet reconstruction and momentum smearing. The beam spectrum was included and the effect of $\gamma\gamma \rightarrow$ hadrons overlay background was added as jet momentum smearing according to CLIC collaboration studies.

The neutral Higgs boson decay through $H \rightarrow b\bar{b}$ was used together with hadronic decay of W bosons to search for the signal events in fully hadronic final state. The charged Higgs masses 250 GeV to 650 GeV were studied with a minimum of 100 GeV mass difference with neutral Higgs bosons to allow $H^+ \rightarrow W^+H$ kinematically.

Results were obtained as invariant mass distributions of charged Higgs boson candidates on top of the SM background followed by a mass window optimization and likelihood analysis.

The conclusion is that although a sizable area is achievable by lepton collider outside the current LHC excluded region, a large coverage is expected by further data from HL-LHC and a lepton collider with $\sqrt{s} = 1400$ GeV only provides a complementary probe of the parameter space but has no discovery potential in the context of the model and process discussed in the paper.

-
- [1] P. W. Higgs, Broken Symmetries and the Masses of Gauge Bosons, *Phys. Rev. Lett.* **13**, 508 (1964).
- [2] P. W. Higgs, Broken symmetries, massless particles and gauge fields, *Phys. Lett.* **12**, 132 (1964).
- [3] F. Englert and R. Brout, Broken Symmetry and the Mass of Gauge Vector Mesons, *Phys. Rev. Lett.* **13**, 321 (1964).
- [4] G. S. Guralnik, C. R. Hagen, and T. W. B. Kibble, Global Conservation Laws and Massless Particles, *Phys. Rev. Lett.* **13**, 585 (1964).
- [5] P. W. Higgs, Spontaneous Symmetry Breakdown without Massless Bosons, *Phys. Rev.* **145**, 1156 (1966).
- [6] T. W. B. Kibble, Symmetry breaking in nonAbelian gauge theories, *Phys. Rev.* **155**, 1554 (1967).
- [7] S. Chatrchyan *et al.* (CMS), Observation of a new boson at a mass of 125 GeV with the CMS experiment at the LHC, *Phys. Lett.* **B716**, 30 (2012), arXiv:1207.7235 [hep-ex].
- [8] G. Aad *et al.* (ATLAS), Observation of a new particle in the search for the Standard Model Higgs boson with the ATLAS detector at the LHC, *Phys. Lett.* **B716**, 1 (2012), arXiv:1207.7214 [hep-ex].
- [9] G. Aad *et al.* (ATLAS), Combined measurements of Higgs boson production and decay using up to 80 fb⁻¹ of proton-proton collision data at $\sqrt{s} = 13$ TeV collected with the ATLAS experiment, *Phys. Rev. D* **101**, 012002 (2020), arXiv:1909.02845 [hep-ex].
- [10] G. Aad *et al.* (ATLAS), CP Properties of Higgs Boson Interactions with Top Quarks in the $t\bar{t}H$ and tH Processes Using $H \rightarrow \gamma\gamma$ with the ATLAS Detector, *Phys. Rev. Lett.* **125**, 061802 (2020), arXiv:2004.04545 [hep-ex].
- [11] G. Aad *et al.* (ATLAS), Test of CP invariance in vector-boson fusion production of the Higgs boson in the $H \rightarrow \tau\tau$ channel in proton-proton collisions at $\sqrt{s} = 13$ TeV with the ATLAS detector, *Phys. Lett. B* **805**, 135426 (2020), arXiv:2002.05315 [hep-ex].
- [12] G. Aad *et al.* (ATLAS), Study of the spin and parity of the Higgs boson in diboson decays with the ATLAS detector, *Eur. Phys. J. C* **75**, 476 (2015), [Erratum:

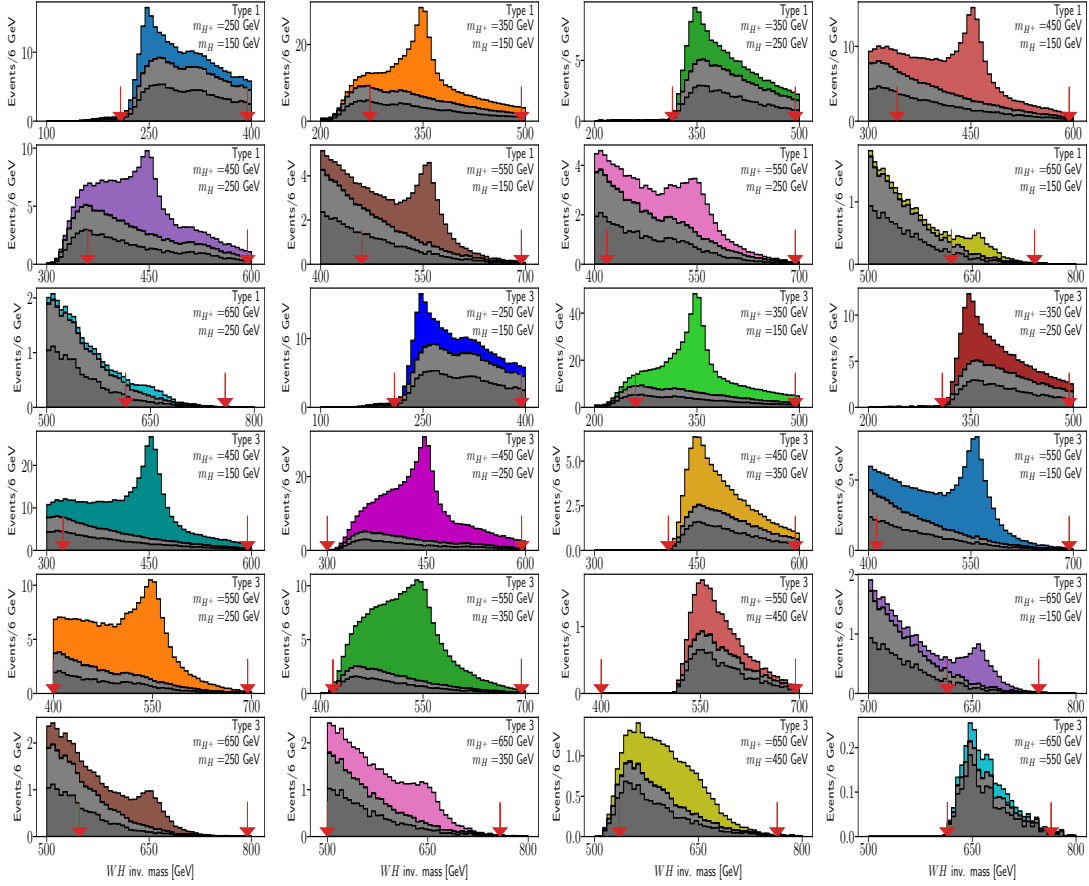


FIG. 13: The charged Higgs candidate invariant mass in 2HDM types 1 and 3 with different mass assumptions at 1000 fb^{-1} .

- Eur.Phys.J.C **76**, 152 (2016)], arXiv:1506.05669 [hep-ex].
- [13] A. M. Sirunyan *et al.* (CMS), Measurement and interpretation of differential cross sections for Higgs boson production at $\sqrt{s} = 13 \text{ TeV}$, Phys. Lett. B **792**, 369 (2019), arXiv:1812.06504 [hep-ex].
- [14] A. M. Sirunyan *et al.* (CMS), Combined measurements of Higgs boson couplings in proton–proton collisions at $\sqrt{s} = 13 \text{ TeV}$, Eur. Phys. J. C **79**, 421 (2019), arXiv:1809.10733 [hep-ex].
- [15] A. M. Sirunyan *et al.* (CMS), Measurements of $t\bar{t}H$ Production and the CP Structure of the Yukawa Interaction between the Higgs Boson and Top Quark in the Diphoton Decay Channel, Phys. Rev. Lett. **125**, 061801 (2020), arXiv:2003.10866 [hep-ex].
- [16] G. Aad *et al.* (ATLAS, CMS), Measurements of the Higgs boson production and decay rates and constraints on its couplings from a combined ATLAS and CMS analysis of the LHC pp collision data at $\sqrt{s} = 7$ and 8 TeV, JHEP **08**, 045, arXiv:1606.02266 [hep-ex].
- [17] M. Carena and H. E. Haber, Higgs Boson Theory and Phenomenology, Prog. Part. Nucl. Phys. **50**, 63 (2003), arXiv:hep-ph/0208209.
- [18] H. Haber and G. Kane, The search for supersymmetry: Probing physics beyond the standard model, Physics Reports **117**, 75 (1985).
- [19] E. M. Dolle and S. Su, The Inert Dark Matter, Phys. Rev. D **80**, 055012 (2009), arXiv:0906.1609 [hep-ph].
- [20] L. Lopez Honorez, E. Nezri, J. F. Oliver, and M. H. G. Tytgat, The Inert Doublet Model: An Archetype for Dark Matter, JCAP **02**, 028, arXiv:hep-ph/0612275.
- [21] M. H. G. Tytgat, The Inert Doublet Model: A New archetype of WIMP dark matter?, J. Phys. Conf. Ser. **120**, 042026 (2008), arXiv:0712.4206 [hep-ph].
- [22] A. Ilnicka, M. Krawczyk, and T. Robens, Inert Doublet Model in light of LHC Run I and astrophysical data, Phys. Rev. D **93**, 055026 (2016), arXiv:1508.01671 [hep-ph].

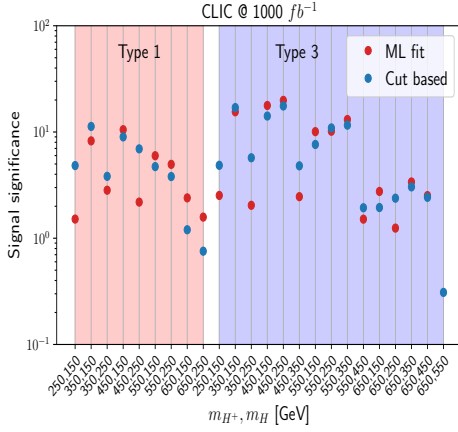


FIG. 14: Comparison of the signal significances obtained from the cut based analysis and the binned maximum likelihood fit.

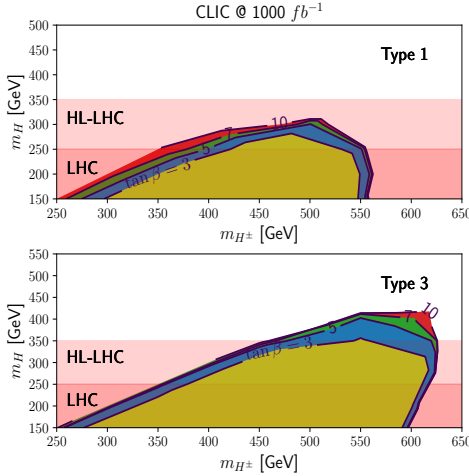


FIG. 15: The 5σ contours of the 2HDM type 1 and 3 at different $\tan\beta$ values. The regions denoted as LHC and HL-LHC show the neutral Higgs excluded regions by the current LHC data and future HL-LHC expectation.

[23] A. Goudelis, B. Herrmann, and O. Stål, Dark matter in the Inert Doublet Model after the discovery of a Higgs-like boson at the LHC, *JHEP* **09**, 106, arXiv:1303.3010 [hep-ph].

[24] E. Lundstrom, M. Gustafsson, and J. Edsjo, The Inert Doublet Model and LEP II Limits, *Phys. Rev. D* **79**, 035013 (2009), arXiv:0810.3924 [hep-ph].

[25] C. Bonilla, D. Sokolowska, N. Darvishi, J. L. Diaz-Cruz, and M. Krawczyk, IDMS: Inert Dark Matter Model with a complex singlet, *J. Phys. G* **43**, 065001 (2016), arXiv:1412.8730 [hep-ph].

[26] J. McDonald, Gauge singlet scalars as cold dark matter, *Phys. Rev. D* **50**, 3637 (1994), arXiv:hep-ph/0702143.

[27] C. P. Burgess, M. Pospelov, and T. ter Veldhuis, The Minimal model of nonbaryonic dark matter: A Sin-

glet scalar, *Nucl. Phys. B* **619**, 709 (2001), arXiv:hep-ph/0011335.

[28] D. O'Connell, M. J. Ramsey-Musolf, and M. B. Wise, Minimal Extension of the Standard Model Scalar Sector, *Phys. Rev. D* **75**, 037701 (2007), arXiv:hep-ph/0611014.

[29] O. Bahat-Treidel, Y. Grossman, and Y. Rozen, Hiding the Higgs at the LHC, *JHEP* **05**, 022, arXiv:hep-ph/0611162.

[30] V. Barger, P. Langacker, M. McCaskey, M. J. Ramsey-Musolf, and G. Shaughnessy, LHC Phenomenology of an Extended Standard Model with a Real Scalar Singlet, *Phys. Rev. D* **77**, 035005 (2008), arXiv:0706.4311 [hep-ph].

[31] X.-G. He, T. Li, X.-Q. Li, and H.-C. Tsai, Scalar dark matter effects in Higgs and top quark decays, *Mod. Phys. Lett. A* **22**, 2121 (2007), arXiv:hep-ph/0701156.

[32] H. Davoudiasl, R. Kitano, T. Li, and H. Murayama, The New minimal standard model, *Phys. Lett. B* **609**, 117 (2005), arXiv:hep-ph/0405097.

[33] V. Barger, P. Langacker, M. McCaskey, M. Ramsey-Musolf, and G. Shaughnessy, Complex Singlet Extension of the Standard Model, *Phys. Rev. D* **79**, 015018 (2009), arXiv:0811.0393 [hep-ph].

[34] R. Coimbra, M. O. P. Sampaio, and R. Santos, ScannerS: Constraining the phase diagram of a complex scalar singlet at the LHC, *Eur. Phys. J. C* **73**, 2428 (2013), arXiv:1301.2599 [hep-ph].

[35] R. Costa, A. P. Morais, M. O. P. Sampaio, and R. Santos, Two-loop stability of singlet extensions of the SM with dark matter, in *2nd Toyama International Workshop on Higgs as a Probe of New Physics* (2015) arXiv:1504.06421 [hep-ph].

[36] M. Gonderinger, H. Lim, and M. J. Ramsey-Musolf, Complex Scalar Singlet Dark Matter: Vacuum Stability and Phenomenology, *Phys. Rev. D* **86**, 043511 (2012), arXiv:1202.1316 [hep-ph].

[37] G.-C. Cho, C. Idegawa, and R. Sugihara, A complex singlet extension of the standard model and multi-critical point principle, *Phys. Lett. B* **839**, 137757 (2023), arXiv:2212.13029 [hep-ph].

[38] J. R. Ellis, G. Gani, and K. A. Olive, Supersymmetric dark matter and the energy of a linear electron positron collider, *Phys. Lett. B* **474**, 314 (2000), arXiv:hep-ph/9912324.

[39] O. Buchmueller, M. Citron, J. Ellis, S. Guha, J. Marrouche, K. A. Olive, K. de Vries, and J. Zheng, Collider Interplay for Supersymmetry, Higgs and Dark Matter, *Eur. Phys. J. C* **75**, 469 (2015), [Erratum: *Eur.Phys.J.C* **76**, 190 (2016)], arXiv:1505.04702 [hep-ph].

[40] S. A. Malik *et al.*, Interplay and Characterization of Dark Matter Searches at Colliders and in Direct Detection Experiments, *Phys. Dark Univ.* **9-10**, 51 (2015), arXiv:1409.4075 [hep-ex].

[41] N. Turok and J. Zadrozny, Dynamical generation of baryons at the electroweak transition, *Phys. Rev. Lett.* **65**, 2331 (1990).

[42] G. Gelmini and M. Roncadelli, Left-handed neutrino mass scale and spontaneously broken lepton number, *Physics Letters B* **99**, 411 (1981).

[43] T. D. Lee, A Theory of Spontaneous T Violation, *Phys. Rev.* **D8**, 1226 (1973).

[44] S. L. Glashow and S. Weinberg, Natural Conservation Laws for Neutral Currents, *Phys. Rev.* **D15**, 1958

- (1977).
- [45] G. C. Branco, Spontaneous CP Nonconservation and Natural Flavor Conservation: A Minimal Model, *Phys. Rev. D* **D22**, 2901 (1980).
- [46] S. Davidson and H. E. Haber, Basis-independent methods for the two-Higgs-doublet model, *Phys. Rev. D* **D72**, 035004 (2005), [Erratum: *Phys. Rev. D* **D72**, 099902(2005)], arXiv:hep-ph/0504050 [hep-ph].
- [47] M. Aoki, S. Kanemura, K. Tsumura, and K. Yagyu, Models of Yukawa interaction in the two Higgs doublet model, and their collider phenomenology, *Phys. Rev. D* **D80**, 015017 (2009), arXiv:0902.4665 [hep-ph].
- [48] T. Aaltonen *et al.* (CDF), High-precision measurement of the W boson mass with the CDF II detector, *Science* **376**, 170 (2022).
- [49] D. López-Val and T. Robens, Δr and the W -boson mass in the singlet extension of the standard model, *Phys. Rev. D* **90**, 114018 (2014), arXiv:1406.1043 [hep-ph].
- [50] D. Lopez-Val and J. Sola, Delta r in the Two-Higgs-Doublet Model at full one loop level – and beyond, *Eur. Phys. J. C* **73**, 2393 (2013), arXiv:1211.0311 [hep-ph].
- [51] C.-T. Lu, L. Wu, Y. Wu, and B. Zhu, Electroweak precision fit and new physics in light of the W boson mass, *Phys. Rev. D* **106**, 035034 (2022), arXiv:2204.03796 [hep-ph].
- [52] H. Bahl, J. Braathen, and G. Weiglein, New physics effects on the W -boson mass from a doublet extension of the SM Higgs sector, *Phys. Lett. B* **833**, 137295 (2022), arXiv:2204.05269 [hep-ph].
- [53] H. Abouabid, A. Arhrib, R. Benbrik, M. Krab, and M. Ouchemhou, Is the new CDF MW measurement consistent with the two-Higgs doublet model?, *Nucl. Phys. B* **989**, 116143 (2023), arXiv:2204.12018 [hep-ph].
- [54] K. Ghorbani and P. Ghorbani, W -boson mass anomaly from scale invariant 2HDM, *Nucl. Phys. B* **984**, 115980 (2022), arXiv:2204.09001 [hep-ph].
- [55] Y. H. Ahn, S. K. Kang, and R. Ramos, Implications of New CDF-II W Boson Mass on Two Higgs Doublet Model, *Phys. Rev. D* **106**, 055038 (2022), arXiv:2204.06485 [hep-ph].
- [56] S. Hossenberger and W. Hollik, Two-loop improved predictions for M_W and $\sin^2\theta_{\text{eff}}$ in Two-Higgs-Doublet models, *Eur. Phys. J. C* **82**, 970 (2022), arXiv:2207.03845 [hep-ph].
- [57] X.-F. Han, F. Wang, L. Wang, J. M. Yang, and Y. Zhang, Joint explanation of W -mass and muon $g-2$ in the 2HDM*, *Chin. Phys. C* **46**, 103105 (2022), arXiv:2204.06505 [hep-ph].
- [58] K. S. Babu, S. Jana, and V. P. K., Correlating W -Boson Mass Shift with Muon $g-2$ in the Two Higgs Doublet Model, *Phys. Rev. Lett.* **129**, 121803 (2022), arXiv:2204.05303 [hep-ph].
- [59] F. J. Botella, F. Cornet-Gomez, C. Miró, and M. Nebot, Muon and electron $g-2$ anomalies in a flavor conserving 2HDM with an oblique view on the CDF M_W value, *Eur. Phys. J. C* **82**, 915 (2022), arXiv:2205.01115 [hep-ph].
- [60] R. Benbrik, M. Boukidi, and B. Manaut, Interpreting the W -Mass and Muon ($g_\mu - 2$) Anomalies within a 2-Higgs Doublet Model, (2022), arXiv:2204.11755 [hep-ph].
- [61] G. Arcadi and A. Djouadi, 2HD plus light pseudoscalar model for a combined explanation of the possible excesses in the CDF MW measurement and $(g-2)_\mu$ with dark matter, *Phys. Rev. D* **106**, 095008 (2022), arXiv:2204.08406 [hep-ph].
- [62] Y. Heo, D.-W. Jung, and J. S. Lee, Impact of the CDF W -mass anomaly on two Higgs doublet model, *Phys. Lett. B* **833**, 137274 (2022), arXiv:2204.05728 [hep-ph].
- [63] S. Lee, K. Cheung, J. Kim, C.-T. Lu, and J. Song, Status of the two-Higgs-doublet model in light of the CDF m_W measurement, *Phys. Rev. D* **106**, 075013 (2022), arXiv:2204.10338 [hep-ph].
- [64] V. D. Barger, J. L. Hewett, and R. J. N. Phillips, New Constraints on the Charged Higgs Sector in Two Higgs Doublet Models, *Phys. Rev. D* **D41**, 3421 (1990).
- [65] G. C. Branco, P. M. Ferreira, L. Lavoura, M. N. Rebelo, M. Sher, and J. P. Silva, Theory and phenomenology of two-Higgs-doublet models, *Phys. Rept.* **516**, 1 (2012), arXiv:1106.0034 [hep-ph].
- [66] E. Ma and D. Ng, New supersymmetric option for two Higgs doublets, *Phys. Rev. D* **D49**, 6164 (1994), arXiv:hep-ph/9305230 [hep-ph].
- [67] S. P. Martin, A Supersymmetry primer, *Adv. Ser. Direct. High Energy Phys.* **18**, 1 (1998), arXiv:hep-ph/9709356.
- [68] I. J. R. Aitchison, Supersymmetry and the MSSM: An Elementary introduction, (2005), arXiv:hep-ph/0505105 [hep-ph].
- [69] A. Djouadi, The Anatomy of electro-weak symmetry breaking. II. The Higgs bosons in the minimal supersymmetric model, *Phys. Rept.* **459**, 1 (2008), arXiv:hep-ph/0503173 [hep-ph].
- [70] J. Bernon, J. F. Gunion, H. E. Haber, Y. Jiang, and S. Kraml, Scrutinizing the alignment limit in two-Higgs-doublet models: $m_h=125$ GeV, *Phys. Rev. D* **92**, 075004 (2015), arXiv:1507.00933 [hep-ph].
- [71] J. Bernon, J. F. Gunion, H. E. Haber, Y. Jiang, and S. Kraml, Scrutinizing the alignment limit in two-Higgs-doublet models. II. $m_H=125$ GeV, *Phys. Rev. D* **93**, 035027 (2016), arXiv:1511.03682 [hep-ph].
- [72] B. Grzadkowski, H. E. Haber, O. M. Ogreid, and P. Osland, Heavy Higgs boson decays in the alignment limit of the 2HDM, *JHEP* **12**, 056, arXiv:1808.01472 [hep-ph].
- [73] P. S. Bhupal Dev and A. Pilaftsis, Natural Alignment in the Two Higgs Doublet Model, *J. Phys. Conf. Ser.* **873**, 012008 (2017), arXiv:1703.05730 [hep-ph].
- [74] J. F. Gunion and H. E. Haber, The CP conserving two Higgs doublet model: The Approach to the decoupling limit, *Phys. Rev. D* **67**, 075019 (2003), arXiv:hep-ph/0207010.
- [75] H. E. Haber, Nonminimal Higgs sectors: The Decoupling limit and its phenomenological implications, in *Joint U.S.-Polish Workshop on Physics from Planck Scale to Electro-Weak Scale (SUSY 94)* (1994) arXiv:hep-ph/9501320.
- [76] M. Misiak *et al.*, Updated NNLO QCD predictions for the weak radiative B-meson decays, *Phys. Rev. Lett.* **114**, 221801 (2015), arXiv:1503.01789 [hep-ph].
- [77] M. Misiak and M. Steinhauser, Weak radiative decays of the B meson and bounds on M_{H^\pm} in the Two-Higgs-Doublet Model, *Eur. Phys. J. C* **77**, 201 (2017), arXiv:1702.04571 [hep-ph].
- [78] M. Misiak, Bounds on M_{H^\pm} from $\bar{B} \rightarrow X_{s,d}\gamma$ Decays, *Acta Phys. Polon. B* **48**, 2173 (2017).
- [79] J. Cardozo, J. H. Muñoz, N. Quintero, and E. Rojas,

- Analysing the charged scalar boson contribution to the charged-current B meson anomalies, *J. Phys. G* **48**, 035001 (2021), arXiv:2006.07751 [hep-ph].
- [80] Y. Amhis *et al.* (HFLAV), Averages of b -hadron, c -hadron, and τ -lepton properties as of summer 2016, *Eur. Phys. J. C* **77**, 895 (2017), arXiv:1612.07233 [hep-ex].
- [81] R. Aaij *et al.* (LHCb), Measurement of the $B_s^0 \rightarrow \mu^+ \mu^-$ branching fraction and effective lifetime and search for $B^0 \rightarrow \mu^+ \mu^-$ decays, *Phys. Rev. Lett.* **118**, 191801 (2017), arXiv:1703.05747 [hep-ex].
- [82] A. M. Sirunyan *et al.* (CMS), Measurement of properties of $B_s^0 \rightarrow \mu^+ \mu^-$ decays and search for $B^0 \rightarrow \mu^+ \mu^-$ with the CMS experiment, *JHEP* **04**, 188, arXiv:1910.12127 [hep-ex].
- [83] M. Aaboud *et al.* (ATLAS), Study of the rare decays of B_s^0 and B^0 mesons into muon pairs using data collected during 2015 and 2016 with the ATLAS detector, *JHEP* **04**, 098, arXiv:1812.03017 [hep-ex].
- [84] F. Mahmoudi and O. Stal, Flavor constraints on the two-Higgs-doublet model with general Yukawa couplings, *Phys. Rev. D* **81**, 035016 (2010), arXiv:0907.1791 [hep-ph].
- [85] R. Aaij *et al.* (LHCb), Measurement of the $B_s^0 \rightarrow \mu^+ \mu^-$ decay properties and search for the $B^0 \rightarrow \mu^+ \mu^-$ and $B_s^0 \rightarrow \mu^+ \mu^- \gamma$ decays, *Phys. Rev. D* **105**, 012010 (2022), arXiv:2108.09283 [hep-ex].
- [86] A. Tumasyan *et al.* (CMS), Measurement of the $B_s^0 \rightarrow \mu^+ \mu^-$ decay properties and search for the $B^0 \rightarrow \mu^+ \mu^-$ decay in proton-proton collisions at $\sqrt{s} = 13$ TeV, *Phys. Lett. B* **842**, 137955 (2023), arXiv:2212.10311 [hep-ex].
- [87] A. Arbey, F. Mahmoudi, O. Stal, and T. Stefaniak, Status of the Charged Higgs Boson in Two Higgs Doublet Models, *Eur. Phys. J. C* **78**, 182 (2018), arXiv:1706.07414 [hep-ph].
- [88] F. Mahmoudi, Overview of the interpretation of indirect searches for charged Higgs bosons in the 2HDM, *PoS CHARGED2016*, 012 (2017).
- [89] F. Mahmoudi, Indirect search for New Physics: complementarity to direct searches, in *25th Rencontres de Blois on Particle Physics and Cosmology* (2013) arXiv:1310.2556 [hep-ph].
- [90] L. Linssen, A. Miyamoto, M. Stanitzki, and H. Weerts, Physics and Detectors at CLIC: CLIC Conceptual Design Report 10.5170/CERN-2012-003 (2012), arXiv:1202.5940 [physics.ins-det].
- [91] H. E. Haber and D. O'Neil, Basis-independent methods for the two-Higgs-doublet model. II. The Significance of $\tan\beta$, *Phys. Rev. D* **74**, 015018 (2006), [Erratum: *Phys. Rev. D* **74**, no.5, 059905(2006)], arXiv:hep-ph/0602242 [hep-ph].
- [92] I. F. Ginzburg and M. Krawczyk, Symmetries of two Higgs doublet model and CP violation, *Phys. Rev. D* **72**, 115013 (2005), arXiv:hep-ph/0408011.
- [93] M. Hashemi and G. Haghigat, Search for neutral Higgs bosons within Type-I 2HDM at future linear colliders, *Eur. Phys. J. C* **79**, 419 (2019), arXiv:1811.11371 [hep-ph].
- [94] M. Hashemi and G. Haghigat, Observability of 2HDM neutral Higgs bosons with different masses at future e^+e^- linear colliders, *Nucl. Phys. B* **951**, 114903 (2020), arXiv:1805.00686 [hep-ph].
- [95] M. Hashemi and G. Haghigat, Capability of future linear colliders to discover heavy neutral CP-even and CP-odd Higgs bosons within Type-I 2HDM, *J. Phys. G* **45**, 095005 (2018), arXiv:1801.02576 [hep-ph].
- [96] M. Hashemi and E. Ebrahimi, Kinematic corrections and reconstruction methods for neutral Higgs boson decay to $b\bar{b}$ in 2HDM type I at future lepton colliders, *Phys. Rev. D* **103**, 115008 (2021), arXiv:2101.00864 [hep-ph].
- [97] M. Hashemi and G. Haghigat, Search for neutral Higgs bosons decaying to $b\bar{b}$ in the flipped 2HDM at future e^-e^+ linear colliders, *Phys. Rev. D* **100**, 015047 (2019), arXiv:1811.12818 [hep-ph].
- [98] M. Hashemi and N. N. Ghalati, Parameter dependence and analysis of the 2HDM neutral Higgs boson pair production and decay at future lepton colliders, *Phys. Lett. B* **830**, 137153 (2022), arXiv:2106.16029 [hep-ph].
- [99] M. Hashemi and M. Molanaei, Heavy neutral 2HDM Higgs boson pair production at CLIC energies, *Phys. Rev. D* **108**, 035012 (2023), arXiv:2306.16116 [hep-ph].
- [100] M. Hashemi, Possibility of observing Higgs bosons at the ILC in the lepton-specific 2HDM, *Phys. Rev. D* **98**, 115004 (2018), arXiv:1805.10513 [hep-ph].
- [101] M. Hashemi, Leptophilic neutral Higgs bosons in two Higgs doublet model at a linear collider, *Eur. Phys. J. C* **77**, 302 (2017), arXiv:1701.02114 [hep-ph].
- [102] M. Hashemi and G. Haghigat, Search for heavy neutral CP-even Higgs within lepton-specific 2HDM at a future linear collider, *Phys. Lett. B* **772**, 426 (2017), arXiv:1704.02940 [hep-ph].
- [103] W. Grimus, L. Lavoura, O. M. Ogreid, and P. Osland, A Precision constraint on multi-Higgs-doublet models, *J. Phys. G* **35**, 075001 (2008), arXiv:0711.4022 [hep-ph].
- [104] J.-M. Gérard and M. Herquet, Twisted custodial symmetry in two-higgs-doublet models, *Phys. Rev. Lett.* **98**, 251802 (2007).
- [105] S. Bertolini, Quantum effects in a two higgs doublet model of the electroweak interactions, *Nuclear Physics B* **272**, 77 (1986).
- [106] A. Denner, R. Guth, and J. Kühn, Relaxation of top mass limits in the two-higgs-doublet model, *Physics Letters B* **240**, 438 (1990).
- [107] J. F. Donoghue and L.-F. Li, Properties of charged higgs bosons, *Phys. Rev. D* **19**, 945 (1979).
- [108] R. M. Godbole and D. P. Roy, Charged-higgs-boson search via heavy-top-quark decay at fermilab tevatron collider energy, *Phys. Rev. D* **43**, 3640 (1991).
- [109] B. K. Bullock, K. Hagiwara, and A. D. Martin, τ polarization as a signal of charged higgs bosons, *Phys. Rev. Lett.* **67**, 3055 (1991).
- [110] D. Roy, Using τ polarization for the charged higgs search at hadron colliders, *Physics Letters B* **277**, 183 (1992).
- [111] S. Raychaudhuri and D. P. Roy, Charged higgs boson search at the fermilab tevatron upgrade using τ polarization, *Phys. Rev. D* **52**, 1556 (1995).
- [112] D. Roy, The hadronic tau decay signature of a heavy charged higgs boson at {LHC}, *Physics Letters B* **459**, 607 (1999).
- [113] S. Raychaudhuri and D. P. Roy, Sharpening up the charged higgs boson signature using τ polarization at the cern lhc, *Phys. Rev. D* **53**, 4902 (1996).
- [114] R. Barate *et al.* (ALEPH), Search for charged Higgs bosons in e^+e^- collisions at energies up to $\sqrt{s} = 189$ GeV, *Phys. Lett. B* **487**, 253 (2000), arXiv:hep-ex/0008005 [hep-ex].
- [115] M. Acciarri *et al.* (L3), Search for charged Higgs bosons

- in e^+e^- collisions at center center-of-mass energies up to 202-GeV, Phys. Lett. **B496**, 34 (2000), arXiv:hep-ex/0009010 [hep-ex].
- [116] Search for charged Higgs bosons: Preliminary combined results using LEP data collected at energies up to 209-GeV, in *Lepton and photon interactions at high energies. Proceedings, 20th International Symposium, LP 2001, Rome, Italy, July 23-28, 2001*.
- [117] B. Abbott *et al.* (D0), Search for charged higgs bosons in decays of top quark pairs, Phys. Rev. Lett. **82**, 4975 (1999), arXiv:hep-ex/9902028 [hep-ex].
- [118] V. M. Abazov *et al.* (D0), Search for charged Higgs bosons in decays of top quarks, Phys. Rev. **D80**, 051107 (2009), arXiv:0906.5326 [hep-ex].
- [119] V. M. Abazov *et al.* (D0), Search for Charged Higgs Bosons in Top Quark Decays, Phys. Lett. **B682**, 278 (2009), arXiv:0908.1811 [hep-ex].
- [120] V. M. Abazov *et al.* (D0), Combination of t anti-t cross section measurements and constraints on the mass of the top quark and its decays into charged Higgs bosons, Phys. Rev. **D80**, 071102 (2009), arXiv:0903.5525 [hep-ex].
- [121] A. Abulencia *et al.* (CDF), Search for charged Higgs bosons from top quark decays in $p\bar{p}$ collisions at $\sqrt{s} = 1.96$ -TeV., Phys. Rev. Lett. **96**, 042003 (2006), arXiv:hep-ex/0510065 [hep-ex].
- [122] G. Yu (CDF), Search for charged Higgs in top quark decays at CDF, *Supersymmetry and the unification of fundamental interactions. Proceedings, 16th International Conference, SUSY08, Seoul, Korea, June 16-21, 2008*, AIP Conf. Proc. **1078**, 198 (2008).
- [123] T. Aaltonen *et al.* (CDF), Search for charged Higgs bosons in decays of top quarks in p anti-p collisions at $\sqrt{s} = 1.96$ TeV, Phys. Rev. Lett. **103**, 101803 (2009), arXiv:0907.1269 [hep-ex].
- [124] M. Baarmand, M. Hashemi, and A. Nikitenko, Light charged Higgs discovery potential of CMS in the $H^\pm \rightarrow \tau\nu_\tau$ decay with single lepton trigger, J. Phys. **G32**, N21 (2006).
- [125] C. Biscarat and M. Dosil, Charged Higgs search in top quark decays with the ATLAS detector, (2003), ATL-PHYS-2003-038, ATL-COM-PHYS-2003-044.
- [126] S. Chatrchyan *et al.* (CMS), Search for a light charged Higgs boson in top quark decays in pp collisions at $\sqrt{s} = 7$ TeV, JHEP **07**, 143, arXiv:1205.5736 [hep-ex].
- [127] S. Chatrchyan *et al.* (CMS), Updated search for a light charged Higgs boson in top quark decays in pp collisions at $\sqrt{s} = 7$ TeV, (2012), CMS-PAS-HIG-12-052.
- [128] G. Aad *et al.* (ATLAS), Search for charged Higgs bosons decaying via $H^+ \rightarrow \tau\nu$ in top quark pair events using pp collision data at $\sqrt{s} = 7$ TeV with the ATLAS detector, JHEP **06**, 039, arXiv:1204.2760 [hep-ex].
- [129] G. Aad *et al.* (ATLAS), Search for a light charged Higgs boson in the decay channel $H^+ \rightarrow c\bar{s}$ in $t\bar{t}$ events using pp collisions at $\sqrt{s} = 7$ TeV with the ATLAS detector, Eur. Phys. J. **C73**, 2465 (2013), arXiv:1302.3694 [hep-ex].
- [130] S. Chatrchyan *et al.* (CMS), Search for charged Higgs bosons with the H^+ to tau nu decay channel in the fully hadronic final state at $\sqrt{s} = 8$ TeV, (2014), CMS-PAS-HIG-14-020.
- [131] G. Aad *et al.* (ATLAS), Search for charged Higgs bosons decaying via $H^\pm \rightarrow \tau^\pm\nu$ in fully hadronic final states using pp collision data at $\sqrt{s} = 8$ TeV with the ATLAS detector, JHEP **03**, 088, arXiv:1412.6663 [hep-ex].
- [132] A. M. Sirunyan *et al.* (CMS), Search for charged Higgs bosons in the $H^\pm \rightarrow \tau^\pm\nu_\tau$ decay channel in proton-proton collisions at $\sqrt{s} = 13$ TeV, JHEP **07**, 142, arXiv:1903.04560 [hep-ex].
- [133] M. Aaboud *et al.* (ATLAS), Search for charged Higgs bosons decaying via $H^\pm \rightarrow \tau^\pm\nu_\tau$ in the τ +jets and τ +lepton final states with 36 fb^{-1} of pp collision data recorded at $\sqrt{s} = 13$ TeV with the ATLAS experiment, JHEP **09**, 139, arXiv:1807.07915 [hep-ex].
- [134] J. L. Diaz-Cruz and O. A. Sampayo, Contribution of gluon fusion to the production of charged higgs bosons at hadron colliders, Phys. Rev. D **50**, 6820 (1994).
- [135] T. Plehn, Charged higgs boson production in bottom-gluon fusion, Phys. Rev. D **67**, 014018 (2003).
- [136] J. Alwall and J. Rathsmann, Improved description of charged higgs boson production at hadron colliders, Journal of High Energy Physics **2004**, 050 (2004).
- [137] N. Kidonakis, Charged higgs production via $bg \rightarrow th^-$ at the lhc, Journal of High Energy Physics **2005**, 011 (2005).
- [138] E. L. Berger, T. Han, J. Jiang, and T. Plehn, Associated production of a top quark and a charged higgs boson, Phys. Rev. D **71**, 115012 (2005).
- [139] K. A. Assamagan, Y. Coadou, and A. Deandrea, ATLAS discovery potential for a heavy charged Higgs boson, Eur. Phys. J.direct **C4**, 9 (2002), arXiv:hep-ph/0203121 [hep-ph].
- [140] K. A. Assamagan and N. Gollub, The ATLAS discovery potential for a heavy charged Higgs boson in $gg \rightarrow tbH^\pm$ with $H^\pm \rightarrow t\bar{b}$, Eur. Phys. J. **C39S2**, 25 (2005), arXiv:hep-ph/0406013 [hep-ph].
- [141] M. Hashemi, Observability of Heavy Charged Higgs through s-channel Single Top Events at LHC, JHEP **11**, 005, arXiv:1310.5209 [hep-ph].
- [142] S. Yang and Q.-S. Yan, Searching for Heavy Charged Higgs Boson with Jet Substructure at the LHC, JHEP **02**, 074, arXiv:1111.4530 [hep-ph].
- [143] J. Gunion, Detecting the tb decays of a charged higgs boson at a hadron supercollider, Physics Letters B **322**, 125 (1994).
- [144] V. D. Barger, R. J. N. Phillips, and D. P. Roy, Heavy charged Higgs signals at the LHC, Phys. Lett. **B324**, 236 (1994), arXiv:hep-ph/9311372 [hep-ph].
- [145] S. Moretti and D. Roy, Detecting heavy charged higgs bosons at the lhc with triple b-tagging, Physics Letters B **470**, 209 (1999).
- [146] M. Hashemi and G. Haghighat, Observability of s-channel Heavy Charged Higgs at LHC Using Top Tagging Technique, JHEP **02**, 040, arXiv:1511.00874 [hep-ph].
- [147] M. Aaboud *et al.* (ATLAS), Search for charged Higgs bosons decaying into top and bottom quarks at $\sqrt{s} = 13$ TeV with the ATLAS detector, JHEP **11**, 085, arXiv:1808.03599 [hep-ex].
- [148] G. Aad *et al.* (ATLAS), Search for charged Higgs bosons decaying into a top quark and a bottom quark at $\sqrt{s} = 13$ TeV with the ATLAS detector, JHEP **06**, 145, arXiv:2102.10076 [hep-ex].
- [149] A. M. Sirunyan *et al.* (CMS), Search for charged Higgs bosons decaying into a top and a bottom quark in the all-jet final state of pp collisions at $\sqrt{s} = 13$ TeV, JHEP **07**, 126, arXiv:2001.07763 [hep-ex].
- [150] A. M. Sirunyan *et al.* (CMS), Search for a charged Higgs

- boson decaying into top and bottom quarks in events with electrons or muons in proton-proton collisions at $\sqrt{s} = 13$ TeV, *JHEP* **01**, 096, arXiv:1908.09206 [hep-ex].
- [151] A. M. Sirunyan *et al.* (CMS), Search for a light charged Higgs boson in the $H^\pm \rightarrow cs$ channel in proton-proton collisions at $\sqrt{s} = 13$ TeV, *Phys. Rev. D* **102**, 072001 (2020), arXiv:2005.08900 [hep-ex].
- [152] A. M. Sirunyan *et al.* (CMS), Search for a charged Higgs boson decaying to charm and bottom quarks in proton-proton collisions at $\sqrt{s} = 8$ TeV, *JHEP* **11**, 115, arXiv:1808.06575 [hep-ex].
- [153] G. Aad *et al.* (ATLAS), Search for a light charged Higgs boson in $t \rightarrow H^\pm b$ decays, with $H^\pm \rightarrow cb$, in the lepton+jets final state in proton-proton collisions at $\sqrt{s} = 13$ TeV with the ATLAS detector, *JHEP* **09**, 004, arXiv:2302.11739 [hep-ex].
- [154] A. Ivina (ATLAS), Search for light charged Higgs boson in $t \rightarrow H^\pm + b(H^\pm \rightarrow cb)$ decays with the ATLAS detector at LHC, PoS **EPS-HEP2021**, 631 (2022).
- [155] M. Hashemi, Observability of Light Charged Higgs Decay to Muon in Top Quark Pair Events at LHC, *Eur. Phys. J. C* **72**, 1994 (2012), arXiv:1109.5356 [hep-ph].
- [156] R. Benbrik, M. Boukidi, B. Manaut, M. Ouchemhou, S. Semlali, and S. Taj, New charged Higgs boson discovery channel at the LHC, (2021), arXiv:2112.07502 [hep-ph].
- [157] P. Bechtle, H. E. Haber, S. Heinemeyer, O. Stål, T. Stefaniak, G. Weiglein, and L. Zeune, The Light and Heavy Higgs Interpretation of the MSSM, *Eur. Phys. J. C* **77**, 67 (2017), arXiv:1608.00638 [hep-ph].
- [158] A. Arhrib, R. Benbrik, and S. Moretti, Bosonic Decays of Charged Higgs Bosons in a 2HDM Type-I, *Eur. Phys. J. C* **77**, 621 (2017), arXiv:1607.02402 [hep-ph].
- [159] H. Bahl, T. Stefaniak, and J. Wittbrodt, The forgotten channels: charged Higgs boson decays to a W^\pm and a non-SM-like Higgs boson, *JHEP* **06**, 183, arXiv:2103.07484 [hep-ph].
- [160] A. Arhrib, R. Benbrik, M. Krab, B. Manaut, S. Moretti, Y. Wang, and Q.-S. Yan, New discovery modes for a light charged Higgs boson at the LHC, *JHEP* **10**, 073, arXiv:2106.13656 [hep-ph].
- [161] R. Enberg, W. Klemm, S. Moretti, S. Munir, and G. Wouda, Search for Charged Higgs bosons via decays to W^\pm and a 125 GeV Higgs at the Large Hadron Collider, PoS **Charged2014**, 027 (2014), arXiv:1502.02931 [hep-ph].
- [162] A. Arhrib, R. Benbrik, and M. Chabab, Charged Higgs bosons decays $H^\pm \rightarrow W^\pm (\gamma, Z)$ revisited, *J. Phys. G* **34**, 907 (2007), arXiv:hep-ph/0607182.
- [163] A. Adhikary, N. Chakraborty, I. Chakraborty, and J. Lahiri, Probing the $H^\pm W^\mp Z$ interaction at the high energy upgrade of the LHC, *Eur. Phys. J. C* **81**, 554 (2021), arXiv:2010.14547 [hep-ph].
- [164] A. Tumasyan *et al.* (CMS), Search for a charged Higgs boson decaying into a heavy neutral Higgs boson and a W boson in proton-proton collisions at $\sqrt{s} = 13$ TeV, *JHEP* **09**, 032, arXiv:2207.01046 [hep-ex].
- [165] A. M. Sirunyan *et al.* (CMS), Search for a light charged Higgs boson decaying to a W boson and a CP-odd Higgs boson in final states with $e\mu\mu$ or $\mu\mu\mu$ in proton-proton collisions at $\sqrt{s} = 13$ TeV, *Phys. Rev. Lett.* **123**, 131802 (2019), arXiv:1905.07453 [hep-ex].
- [166] J. H. Bhyun (CMS), Search for a light charged Higgs boson decaying to a W boson and a CP-odd Higgs boson in trilepton final states in pp collisions at 13 TeV with CMS, PoS **ICHEP2020**, 095 (2021).
- [167] A. M. Sirunyan *et al.* (CMS), Search for Charged Higgs Bosons Produced via Vector Boson Fusion and Decaying into a Pair of W and Z Bosons Using pp Collisions at $\sqrt{s} = 13$ TeV, *Phys. Rev. Lett.* **119**, 141802 (2017), arXiv:1705.02942 [hep-ex].
- [168] M. Aaboud *et al.* (ATLAS), Search for resonant WZ production in the fully leptonic final state in proton-proton collisions at $\sqrt{s} = 13$ TeV with the ATLAS detector, *Phys. Lett. B* **787**, 68 (2018), arXiv:1806.01532 [hep-ex].
- [169] G. Aad *et al.* (ATLAS), Search for doubly and singly charged Higgs bosons decaying into vector bosons in multi-lepton final states with the ATLAS detector using proton-proton collisions at $\sqrt{s} = 13$ TeV, *JHEP* **06**, 146, arXiv:2101.11961 [hep-ex].
- [170] G. Aad *et al.* (ATLAS), Search for doubly and singly charged Higgs bosons decaying into vector bosons in multi-lepton final states with the ATLAS detector using proton-proton collisions at $\sqrt{s} = 13$ TeV, *JHEP* **06**, 146, arXiv:2101.11961 [hep-ex].
- [171] M. Cepeda *et al.*, Report from Working Group 2: Higgs Physics at the HL-LHC and HE-LHC, CERN Yellow Rep. Monogr. **7**, 221 (2019), arXiv:1902.00134 [hep-ph].
- [172] H. Bahl, P. Bechtle, S. Heinemeyer, S. Liebler, T. Stefaniak, and G. Weiglein, HL-LHC and ILC sensitivities in the hunt for heavy Higgs bosons, *Eur. Phys. J. C* **80**, 916 (2020), arXiv:2005.14536 [hep-ph].
- [173] A. Abada *et al.* (FCC), FCC-hh: The Hadron Collider: Future Circular Collider Conceptual Design Report Volume 3, *Eur. Phys. J. ST* **228**, 755 (2019).
- [174] A. Abada *et al.* (FCC), FCC-ee: The Lepton Collider: Future Circular Collider Conceptual Design Report Volume 2, *Eur. Phys. J. ST* **228**, 261 (2019).
- [175] I. Agapov *et al.*, Future Circular Lepton Collider FCC-ee: Overview and Status, in *Snowmass 2021* (2022) arXiv:2203.08310 [physics.acc-ph].
- [176] P. Bambade *et al.*, The International Linear Collider: A Global Project, (2019), arXiv:1903.01629 [hep-ex].
- [177] T. Barklow, J. Brau, K. Fujii, J. Gao, J. List, N. Walker, and K. Yokoya, ILC Operating Scenarios, (2015), arXiv:1506.07830 [hep-ex].
- [178] J. E. Brau, T. Barklow, J. Brau, K. Fujii, J. Gao, J. List, N. Walker, and K. Yokoya (ILC Parameters Joint Working Group), 500 GeV ILC Operating Scenarios, in *Meeting of the APS Division of Particles and Fields* (2015) arXiv:1510.05739 [hep-ex].
- [179] The CEPC input for the European Strategy for Particle Physics - Physics and Detector, (2019), arXiv:1901.03170 [hep-ex].
- [180] M. Dong *et al.* (CEPC Study Group), CEPC Conceptual Design Report: Volume 2 - Physics & Detector, (2018), arXiv:1811.10545 [hep-ex].
- [181] A. Abada *et al.* (FCC), FCC Physics Opportunities: Future Circular Collider Conceptual Design Report Volume 1, *Eur. Phys. J. C* **79**, 474 (2019).
- [182] D. M. Asner *et al.*, ILC Higgs White Paper, in *Community Summer Study 2013: Snowmass on the Mississippi* (2013) arXiv:1310.0763 [hep-ph].
- [183] F. An *et al.*, Precision Higgs physics at the CEPC, *Chin. Phys. C* **43**, 043002 (2019), arXiv:1810.09037 [hep-ex].
- [184] H. Abramowicz *et al.*, Higgs physics at the CLIC elec-

- tron-positron linear collider, *Eur. Phys. J. C* **77**, 475 (2017), arXiv:1608.07538 [hep-ex].
- [185] Higgs physics at clic, *Nuclear and Particle Physics Proceedings* **273-275**, 801 (2016), 37th International Conference on High Energy Physics (ICHEP).
- [186] D. Eriksson, J. Rathsmann, and O. Stal, 2HDMC: Two-Higgs-Doublet Model Calculator Physics and Manual, *Comput. Phys. Commun.* **181**, 189 (2010), arXiv:0902.0851 [hep-ph].
- [187] D. Eriksson, J. Rathsmann, and O. Stal, 2HDMC: Two-Higgs-doublet model calculator, *Comput. Phys. Commun.* **181**, 833 (2010).
- [188] R. Harlander, M. Mühleitner, J. Rathsmann, M. Spira, and O. Stål, Interim recommendations for the evaluation of Higgs production cross sections and branching ratios at the LHC in the Two-Higgs-Doublet Model, (2013), arXiv:1312.5571 [hep-ph].
- [189] H. Bahl, T. Biekötter, S. Heinemeyer, C. Li, S. Paasch, G. Weiglein, and J. Wittbrodt, HiggsTools: BSM scalar phenomenology with new versions of HiggsBounds and HiggsSignals, *Comput. Phys. Commun.* **291**, 108803 (2023), arXiv:2210.09332 [hep-ph].
- [190] W. Kilian, T. Ohl, and J. Reuter, WHIZARD: Simulating Multi-Particle Processes at LHC and ILC, *Eur. Phys. J. C* **71**, 1742 (2011), arXiv:0708.4233 [hep-ph].
- [191] M. Moretti, T. Ohl, and J. Reuter, O'Mega: An Optimizing matrix element generator, *JHEP*, 1981 (2001), arXiv:hep-ph/0102195.
- [192] T. Ohl, CIRCE version 1.0: Beam spectra for simulating linear collider physics, *Comput. Phys. Commun.* **101**, 269 (1997), arXiv:hep-ph/9607454.
- [193] T. Sjostrand, S. Mrenna, and P. Z. Skands, A Brief Introduction to PYTHIA 8.1, *Comput. Phys. Commun.* **178**, 852 (2008), arXiv:0710.3820 [hep-ph].
- [194] J. de Favereau, C. Delaere, P. Demin, A. Giammanco, V. Lemaitre, A. Mertens, and M. Selvaggi (DELPHES 3), DELPHES 3, A modular framework for fast simulation of a generic collider experiment, *JHEP* **02**, 057, arXiv:1307.6346 [hep-ex].
- [195] M. Selvaggi, DELPHES 3: A modular framework for fast-simulation of generic collider experiments, *J. Phys. Conf. Ser.* **523**, 012033 (2014).
- [196] A. Mertens, New features in Delphes 3, *J. Phys. Conf. Ser.* **608**, 012045 (2015).
- [197] D. Arominski *et al.* (CLICdp), A detector for CLIC: main parameters and performance, (2018), arXiv:1812.07337 [physics.ins-det].
- [198] E. Leogrande, P. Roloff, U. Schnoor, and M. Weber, A DELPHES card for the CLIC detector, (2019), arXiv:1909.12728 [hep-ex].
- [199] N. Alipour Tehrani *et al.* (CLICdp), CLICdet: The post-CDR CLIC detector model, (2017), CLICdp-Note-2017-001.
- [200] R. Brun and F. Rademakers, ROOT: An object oriented data analysis framework, *New computing techniques in physics research V. Proceedings, 5th International Workshop, AIHENP '96, Lausanne, Switzerland, September 2-6, 1996*, *Nucl. Instrum. Meth.* **A389**, 81 (1997).
- [201] C. R. Harris, K. J. Millman, S. J. van der Walt, R. Gommers, P. Virtanen, D. Cournapeau, E. Wieser, J. Taylor, S. Berg, N. J. Smith, R. Kern, M. Picus, S. Hoyer, M. H. van Kerkwijk, M. Brett, A. Haldane, J. F. del Río, M. Wiebe, P. Peterson, P. Gérard-Marchant, K. Sheppard, T. Reddy, W. Weckesser, H. Abbasi, C. Gohlke, and T. E. Oliphant, Array programming with NumPy, *Nature* **585**, 357 (2020).
- [202] J. D. Hunter, Matplotlib: A 2d graphics environment, *Computing in Science & Engineering* **9**, 90 (2007).
- [203] I. F. Ginzburg and I. P. Ivanov, Tree level unitarity constraints in the 2HDM with CP violation, (2003), arXiv:hep-ph/0312374.
- [204] N. G. Deshpande and E. Ma, Pattern of Symmetry Breaking with Two Higgs Doublets, *Phys. Rev. D* **18**, 2574 (1978).
- [205] B. M. Kastening, Bounds from stability and symmetry breaking on parameters in the two Higgs doublet potential, (1992), arXiv:hep-ph/9307224.
- [206] J. F. Gunion and H. E. Haber, The CP conserving two Higgs doublet model: The Approach to the decoupling limit, *Phys. Rev. D* **67**, 075019 (2003), arXiv:hep-ph/0207010.
- [207] A. Arhrib, Unitarity constraints on scalar parameters of the standard and two Higgs doublets model, in *Workshop on Noncommutative Geometry, Superstrings and Particle Physics* (2000) arXiv:hep-ph/0012353.
- [208] I. F. Ginzburg and I. P. Ivanov, Tree level unitarity constraints in the 2HDM with CP violation, (2003), arXiv:hep-ph/0312374.
- [209] M. Aaboud *et al.* (ATLAS), Search for a heavy Higgs boson decaying into a Z boson and another heavy Higgs boson in the $\ell b b$ final state in pp collisions at $\sqrt{s} = 13$ TeV with the ATLAS detector, *Phys. Lett. B* **783**, 392 (2018), arXiv:1804.01126 [hep-ex].
- [210] Searches for additional Higgs bosons and for vector leptoquarks in $\tau\tau$ final states in proton-proton collisions at $\sqrt{s} = 13$ TeV, CMS Collaboration, CMS-HIG-21-001, CERN-EP-2022-137 (2022), arXiv:2208.02717 [hep-ex].
- [211] M. Aaboud *et al.* (ATLAS), Search for low-mass resonances decaying into two jets and produced in association with a photon using pp collisions at $\sqrt{s} = 13$ TeV with the ATLAS detector, *Phys. Lett. B* **795**, 56 (2019), arXiv:1901.10917 [hep-ex].
- [212] G. Aad *et al.* (ATLAS), Search for heavy Higgs bosons decaying into two tau leptons with the ATLAS detector using pp collisions at $\sqrt{s} = 13$ TeV, *Phys. Rev. Lett.* **125**, 051801 (2020), arXiv:2002.12223 [hep-ex].
- [213] V. Khachatryan *et al.* (CMS), Search for neutral resonances decaying into a Z boson and a pair of b jets or τ leptons, *Phys. Lett. B* **759**, 369 (2016), arXiv:1603.02991 [hep-ex].
- [214] G. Aad *et al.* (ATLAS), Search for neutral Higgs bosons of the minimal supersymmetric standard model in pp collisions at $\sqrt{s} = 8$ TeV with the ATLAS detector, *JHEP* **11**, 056, arXiv:1409.6064 [hep-ex].
- [215] A. Muennich, TauFinder: A Reconstruction Algorithm for τ Leptons at Linear Colliders, LCD-Note-2010-009 (2010).
- [216] N. Alipour Tehrani and P. Roloff, Optimisation Studies for the CLIC Vertex-Detector Geometry, CLICdp-Note-2014-002 (2014).
- [217] S. D. Drell and T.-M. Yan, Massive lepton-pair production in hadron-hadron collisions at high energies, *Phys. Rev. Lett.* **25**, 316 (1970).
- [218] S. D. Drell and T.-M. Yan, Massive lepton-pair production in hadron-hadron collisions at high energies, *Phys. Rev. Lett.* **25**, 902 (1970).
- [219] M. Boronat, J. Fuster, I. Garcia, E. Ros, and

- M. Vos, A robust jet reconstruction algorithm for high-energy lepton colliders, *Phys. Lett. B* **750**, 95 (2015), arXiv:1404.4294 [hep-ex].
- [220] M. Boronat, J. Fuster, I. Garcia, P. Roloff, R. Simoniello, and M. Vos, Jet reconstruction at high-energy electron–positron colliders, *Eur. Phys. J. C* **78**, 144 (2018), arXiv:1607.05039 [hep-ex].
- [221] J. M. Butterworth, A. R. Davison, M. Rubin, and G. P. Salam, Jet substructure as a new Higgs search channel at the LHC, *Phys. Rev. Lett.* **100**, 242001 (2008), arXiv:0802.2470 [hep-ph].
- [222] T. Plehn and M. Spannowsky, Top Tagging, *J. Phys.* **G39**, 083001 (2012), arXiv:1112.4441 [hep-ph].
- [223] D. E. Kaplan, K. Rehermann, M. D. Schwartz, and B. Tweedie, Top Tagging: A Method for Identifying Boosted Hadronically Decaying Top Quarks, *Phys. Rev. Lett.* **101**, 142001 (2008), arXiv:0806.0848 [hep-ph].
- [224] T. Plehn, G. P. Salam, and M. Spannowsky, Fat Jets for a Light Higgs, *Phys. Rev. Lett.* **104**, 111801 (2010), arXiv:0910.5472 [hep-ph].